minerals

MDPI

Review

Review of Enargite Flotation—Part I: Surface Characterization and Advances in Selective Flotation

Pablo Miranda-Villagrán [1], Rodrigo Yepsen [1], Andrés Ramírez-Madrid [1,2], Jorge H. Saavedra [3] and Leopoldo Gutiérrez [1,2,*]

[1] Department of Metallurgical Engineering, University of Concepcion, Concepción 4070409, Chile; pamiranda@udec.cl (P.M.-V.); rodrigoyepsen@udec.cl (R.Y.); aramirezm@udec.cl (A.R.-M.)
[2] Water Research Center for Agriculture and Mining (CRHIAM), University of Concepcion, Concepción 4070409, Chile
[3] Department of Wood Engineering, Universidad del Bío-Bío, Concepción 4081112, Chile; jsaavedra@ubiobio.cl
* Correspondence: lgutierrezb@udec.cl

Abstract

Enargite (Cu_3AsS_4), a copper–arsenic sulfosalt, represents a critical challenge in copper mineral processing due to its high arsenic content, which poses significant environmental, metallurgical, and economic issues. Its flotation behavior closely resembles that of other copper sulfides such as chalcopyrite and chalcocite, complicating selective separation at early beneficiation stages. This review presents a comprehensive examination of enargite's surface chemistry and electrochemical behavior, focusing on the influence of oxidation, pH, and pulp potential on surface reactivity, charge distribution (zeta potential), and hydrophobicity. Detailed insights into the formation of surface oxidation layers, passivation mechanisms, and contact angle variations are provided to elucidate collector-mineral interactions. Advances in selective flotation techniques are also discussed, including the use of depressant reagents, controlled redox environments, and reagent conditioning strategies. Special attention is given to flotation in seawater, where ionic strength and multivalent ions significantly influence mineral-reagent interactions and flotation outcomes. Galvanic interactions between enargite and other sulfide minerals are identified as critical factors affecting floatability and selectivity. The review consolidates findings from recent experimental and electrochemical studies, highlighting promising approaches to enhance enargite rejection and copper concentrate purity. It concludes with perspectives on future research aimed at optimizing flotation processes and developing sustainable solutions for processing arsenic-bearing copper ores.

Keywords: enargite; flotation; copper minerals; arsenic minerals

Academic Editor: Wengang Liu

Received: 22 July 2025
Revised: 25 August 2025
Accepted: 10 September 2025
Published: 13 September 2025

Citation: Miranda-Villagrán, P.; Yepsen, R.; Ramírez-Madrid, A.; Saavedra, J.H.; Gutiérrez, L. Review of Enargite Flotation—Part I: Surface Characterization and Advances in Selective Flotation. *Minerals* **2025**, *15*, 971. https://doi.org/10.3390/min15090971

1. Introduction

Enargite (Cu_3AsS_4) is one of the most problematic arsenical minerals in copper deposits, mainly because of its association with non-arsenic copper sulfides such as chalcopyrite ($CuFeS_2$) and chalcocite (Cu_2S) [1,2]. Enargite in copper concentrates generates serious environmental and health problems due to the release of arsenic during smelting processes, leading to economic penalties when the arsenic content exceeds 0.2% [3], posing challenges for selectively concentrating copper sulfides, since their interaction mechanisms with collectors are similar to those of enargite. In addition to its environmental implications, arsenic affects the physical properties of copper, such as its electrical conductivity, making it an undesirable contaminant in copper concentrates [4,5].

Separating enargite from other copper sulfides in the early processing stages, such as flotation, is very important to mitigate these problems. However, achieving selective flotation between enargite and other copper sulfides is challenging due to the similar surface properties exhibited by these minerals when conventional thiol-type collectors such as xanthates are employed [6]. The effective flotation separation of enargite from other copper sulfides strongly depends on its surface properties, including enargite's chemical surface properties, zeta potential, the influence of electrochemical potential on surface characteristics, and contact angle under varying physicochemical conditions.

Several strategies have been explored for the selective flotation of enargite, including the use of pulp potential control, the use of specific reagents for selective oxidation of enargite, and selective flotation reagents [7,8]. Among these approaches, pulp potential–controlled flotation has been extensively investigated, whereas fewer studies address the effects of selective oxidation and selective depressant reagents on this process [9]. On the other hand, in recent years, the use of seawater in mineral processing has received increasing attention due to the growing scarcity of freshwater in mining regions. Nevertheless, the application of seawater in flotation processes presents additional challenges, as the presence of various ions can affect both the floatability of minerals and the interaction mechanisms of flotation reagents [10].

This review article, particularly in Sections 2 and 3, presents the most recent advances in the study of the surface properties of enargite, as well as the development of strategies to achieve its selective flotation from other copper sulfides. These chapters summarize key findings related to surface chemistry, electrochemical behavior, and flotation response under various conditions. Finally, Section 4 outlines prospects for future research, focusing on addressing current challenges, improving the understanding of enargite-reagent interactions, and optimizing flotation processes to enhance the selectivity and efficiency of enargite separation.

2. Surface and Electrochemical Properties of Enargite

2.1. Chemical Surface Properties

Enargite is a copper–arsenic sulfosalt mineral that exhibits a unique and complex crystal structure, making it a subject of considerable interest in both mineralogical and metallurgical studies. Understanding its atomic arrangement is essential, since the geometry and bonding environment of its constituent atoms influence not only its stability but also its reactivity in various processes, such as flotation and leaching. Enargite forms a wurtzite-type superstructure with a distorted close-packed hexagonal array of sulfur atoms. Copper and arsenic atoms, in a 3:1 ratio, occupy only half of the available tetrahedral sites (Figure 1). Each cation coordinates tetrahedrally with four sulfur atoms, while each sulfur atom coordinates with one arsenic atom and three copper atoms. The tetrahedra surrounding arsenic appear smaller and more regular, with angles close to 109.5°. This tetrahedral configuration is uncommon in arsenosulfide compounds, where trigonal–pyramidal coordination predominates [11].

Alterations of the chemical surface properties of enargite, which in turn control the adsorption of collectors, hydrophobicity and the ability of the enargite particles to attach to air bubbles during flotation. This is why understanding the behavior of enargite's atomic structure under varying physicochemical conditions is crucial for elucidating its surface properties. In addition, changes at the atomic level—such as elemental migration, bond rearrangement, or surface reconstruction—can significantly influence key factors like surface charge, reactivity, and interaction with flotation reagents, all of which directly impact its flotation performance.

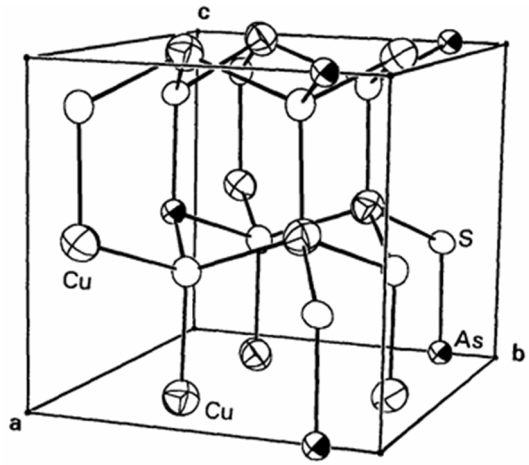

Figure 1. Crystal structure of enargite, Cu_3AsS_4 (ref. [11] with permission).

Vaughan et al. [12] described the surface chemistry and the initial reactions of oxidation in sulfide minerals using X-ray absorption spectroscopy (XAS) and X-ray photoelectron spectroscopy (XPS). The study highlighted that copper sulfides exhibit a surface relaxation similar to that observed in sphalerite in which Zn atoms shift toward the solid interior while S atoms migrate toward the surface. Rosso et al. [13,14] supported these results and reported that enargite has a structure based on the wurtzite form of ZnS, in which Cu and one-quarter replace three-quarters of the Zn by As. Additionally, all atoms are in tetrahedral coordination, and the AsS_4 tetrahedra do not share any of their S atoms.

Rossi et al. [15] characterized the surface chemical composition of enargite using XPS. The research results revealed the formation of an oxidized film of approximately 0.5 nm of thickness on the mineral surface after exposure to the atmosphere, which showed significant arsenic enrichment and the presence of copper oxide or sulfate, as suggested by previous studies [16,17]. The detection of $CuSO_4$ and As_2O_x (x = 3, 5) is consistent with other electrochemical oxidation studies [18,19]. Additionally, a subsurface layer enriched in copper and depleted in sulfur was identified, indicating the segregation of arsenic and sulfur to the surface during the oxidation process. Any further investigation into the interaction of enargite with the environment must consider the presence of this oxidized surface layer and its influence on the mineral's stability and reactivity in aqueous environments.

Pratt et al. [20] studied the surface and subsurface chemistry of enargite after it was fractured under ultra-high vacuum conditions using XPS and synchrotron radiation X-ray photoelectron spectroscopy (SRXPS). They showed that the enargite surface reorganizes after fracturing, with arsenic atoms extended on the surface. The As 3D data revealed that surface arsenic atoms had an energy level approximately 1 eV lower than arsenic atoms in the mineral matrix, suggesting surface reconfiguration that highlights the prominence of arsenic after fracturing. Sulfur showed no significant differences between the surface and the mineral matrix. Additionally, copper atoms were found in the cuprous state (Cu^+).

In summary, the studies show that when enargite is exposed to air it forms an arsenic-rich oxidized layer with copper oxides and sulfates, altering surface charge and reactivity. These changes affect collector adsorption and bubble attachment. Enargite's wurtzite-type structure and surface reorganization upon fracture also influence its interaction with flotation reagents. Understanding these processes is key to improving flotation performance and reagent selection.

2.2. Zeta Potential

Understanding the zeta potential of enargite and its relationship with surface oxidation mechanisms is essential for optimizing enargite flotation and enhancing its selectivity with respect to other metal sulfides. Zeta potential, which indirectly reflects the surface charge of mineral particles, varies with pH and plays a crucial role in influencing particle dispersion or aggregation, as well as the mineral's affinity for flotation reagents. The zeta potential of enargite strongly depends on pH, which also influences the adsorption of collectors on the particle's surfaces, thereby affecting its hydrophobicity and ability to attach to air bubbles which is critical for selective separation. Zeta potential and pH relate to the formation of oxide layers on the mineral surface that can significantly alter its floatability, highlighting the importance of understanding the surface properties of enargite and their interaction with key parameters such as pH and oxidation state [21,22].

Fullston et al. [23] studied the surface oxidation of enargite by following metal dissolution and changes in the zeta potential under different oxidizing conditions (Figure 2). The results indicated that enargite treated with high-purity water, adjusted to pH 11.0, using KNO_3 as the supporting electrolyte and conditioned under nitrogen atmosphere, exhibited a consistently negative zeta potential ranging from −40 mV/SHE at pH 5.0 to −60 mV at pH 11.0. However, when enargite was conditioned with oxygen, the zeta potential curves became less negative and positive when pH went from low to high values. In contrast, the results by Fullston et al. [23] presented in Figure 1 also reveal a significant difference in the zeta potential when the pH was adjusted from high to low values. These results highlight the dependence of the surface state on both the current pH of the solution and previous pH adjustments. This hysteresis phenomenon was attributed to the dissolution of copper from the mineral structure at acidic pH levels and under oxidizing conditions, which is reflected in an increased concentration of copper in the solution.

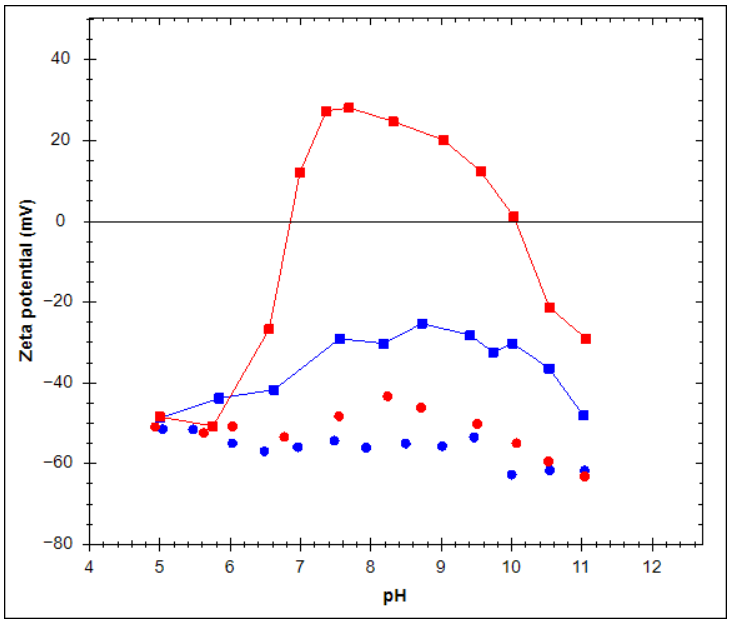

Figure 2. Zeta potential versus pH of natural enargite conditioned at pH 11 for 20 min in nitrogen (circle), and 60 min in oxygen (square). Blue and red symbols refer to a pH change from high to low and low to high values, respectively (Adapted from [23]).

The understanding of the hysteresis phenomenon can be integrated with previous studies that proposed that, in acidic solutions, copper migrates to the surface and dissolves, whereas in alkaline environments, a layer of metal hydroxide forms on a sulfur-rich surface. These oxidation and surface charge formation mechanisms provide a broader

context for understanding the electrochemical interactions and reactivity of enargite under different conditions [24–28]. Reactions 1 and 2 illustrate schemes for the protonation and deprotonation of metal sulfide surfaces within this framework.

$$-\mathrm{MSH} + \mathrm{H}^+ \leftrightarrow -\mathrm{MSH}_2^+ \quad / \quad -\mathrm{MSH} \leftrightarrow \mathrm{MS}^- + \mathrm{H}^+ \tag{1}$$

$$-\mathrm{MOH} + \mathrm{H}^+ \leftrightarrow -\mathrm{MOH}_2^+ \quad / \quad -\mathrm{MOH} \leftrightarrow \mathrm{MO}^- + \mathrm{H}^+ \tag{2}$$

Previous studies showed that the sulfur-rich surface of enargite consists of a metal-deficient sulfide, polysulfide, or elemental sulfur structure depending on the degree of oxidation [29]. This causes the zeta potential to become more negative as the pH increases. As oxidation progresses, sulfide groups are transformed into polysulfides or elemental sulfur. In the presence of oxygen and high pH, hydrolysis and precipitation of metal hydroxides occur on the sulfur-rich surface, altering the surface charge. Changes in zeta potential with pH and oxidizing conditions are consistent with this copper hydroxide layer covering the sulfur-rich, metal-deficient surface, with the extent of this copper hydroxide coverage increasing under oxidizing conditions [30].

Concerning metal dissolution, it was reported that copper dissolved more extensively than arsenic in alkaline conditions. However, under more acidic conditions and in the presence of ferric ions, the dissolution rates of copper and arsenic were found to be similar. The variations in the zeta potential of enargite as a function of pH under oxidizing conditions, reported by [23], showed similar trends to those described for other copper sulfide minerals, such as chalcocite [31,32]. In a more detailed analysis, Fullston et al. [33] using XPS reported that the oxidation layer on the surface of enargite includes copper and arsenic oxides/hydroxides, sulfite, and a sulfur-rich layer composed of metal-deficient sulfide and/or polysulfides. The proportion of all these oxidation products on the mineral surface is more significant when it is treated under more oxidizing conditions. Additionally, arsenic sulfide species, such as As_4S_4 or As_2S_3, were also found on the surface of enargite, and their presence was not related to surface impurities in the enargite sample, as confirmed by Córdoba et al. [34].

Castro and Honores [35], using micro-electrokinetic measurements and microflotation tests, investigated the surface properties of enargite at different pH values. These authors found that the zeta potentials were negative (−21 to −47 mV) in the pH range between 2.5 and 12.0 with no isoelectric point. Peaks of potential were observed around pH 5.5 and 11.0, as shown in Figure 3. It was argued that these peaks could be explained by the presence of arsenate ions $(AsO_4)^{3-}$ resulting from the surface dissolution of enargite which was confirmed by investigating the effect of adding sodium arsenate. Schwedt and Rieckhoff [36] reported that the observed potential peaks corresponded to the hydrolysis of arsenate and thioarsenate ions, reflecting similar pK values. Based on this study, it was suggested that the negative zeta potential of enargite could be explained by the presence of negatively charged thioarsenate species formed from acids such as arsenic acid (H_3AsO_4), thioarsenic acid (H_3AsO_3S), dithioarsenic acid ($H_3AsO_2S_2$), and trithioarsenic acid (H_3AsOS_3). By comparing the rest potentials with the Eh–pH diagrams of the As–Cu–S–H_2O and Cu–As–S–H_2O systems (Figure 4), it was suggested that under alkaline conditions, enargite tends to dissolve, favoring the formation of arsenate ions [35]. In the same alkaline range, the formation of $Cu(OH)_2$ is observed, suggesting the creation of an oxide surface layer that limits its direct dissolution into the medium. Under acidic conditions, the generation of an arsenic trioxide surface layer, represented as the anhydride form of arsenious acid, is expected. This behavior contrasts with copper sulfides, which form an oxide layer in alkaline media and dissolve under acidic conditions.

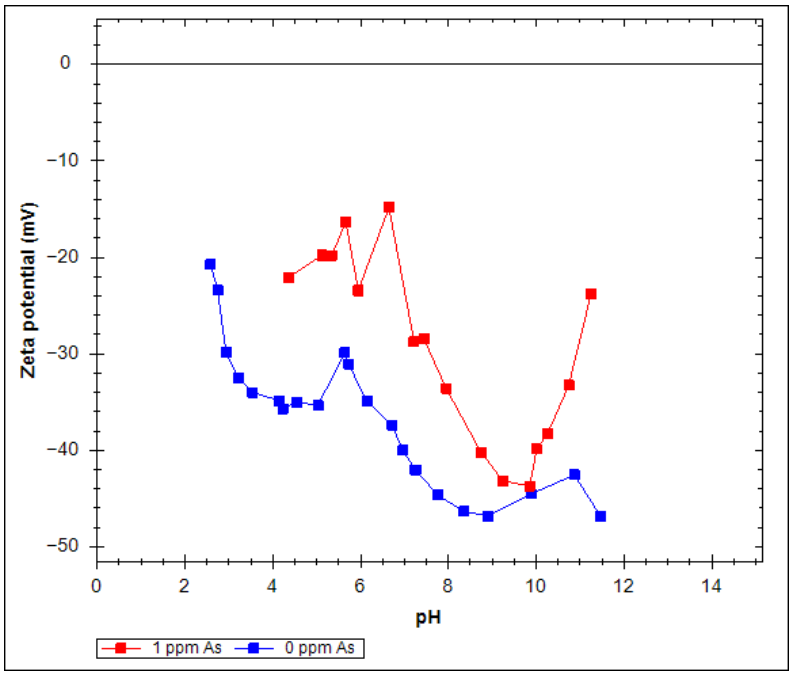

Figure 3. Zeta potential of enargite as a function of pH in the presence and absence of arsenate ions in a 10^{-3} M $NaNO_3$ supporting electrolyte (Adapted from [35]).

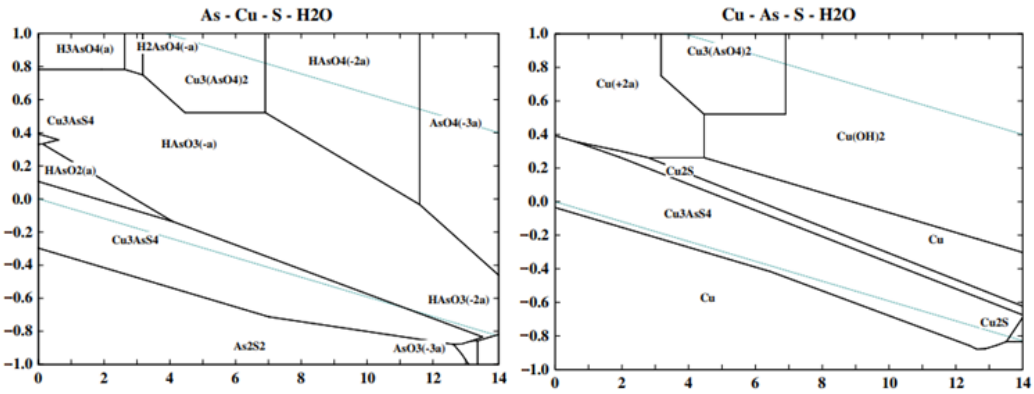

Figure 4. Left: Eh–pH diagrams for the As–Cu–S–H_2O system at 278 K. Right: Eh–pH diagrams for the Cu–As–S–H_2O system at 278 K. A dissolved copper activity of 3×10^{-3} M is assumed. The vertical and horizontal axes represent the redox potential (Eh) in V/SHE and the solution pH, respectively, while the dashed lines indicate the upper and lower limits of water stability (ref. [37] with permission).

Castro and Baltierra [38] investigated the effect of pH on the zeta potential of enargite using two different supporting electrolytes. Their findings confirmed that enargite exhibits a consistently negative zeta potential across the entire pH range studied without displaying an isoelectric point. As shown in Figure 5, unusual peaks were observed in the zeta potential curves: one around pH 5.5 for both electrolytes, and a second that varied depending on the electrolyte—at pH 9.5 with sodium nitrate ($NaNO_3$) and at pH 11.0 with potassium chloride (KCl). These peaks were related to the arsenic surface chemistry, suggesting the formation of hydrolysis products such as thioarsenic and oxothioarsenic acids on the enargite surface. It was proposed that the lowest zeta potential values coincided with the highest concentrations of $H_2AsO_4^-$ and $HAsO_4^{2-}$ ions, indicating that the dissociation of these species may significantly influence the zeta potential of enargite.

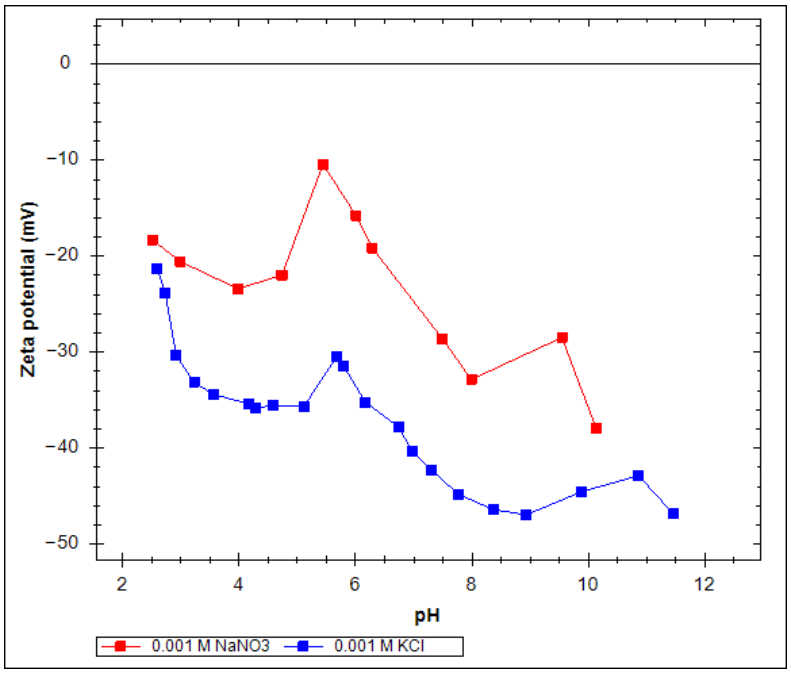

Figure 5. Zeta potential of enargite as a function of pH (Adapted from [38]).

The influence of flotation reagent adsorption on the zeta potential of enargite should be considered in conjunction with the surface oxidation processes that govern the nature of species present at the mineral–solution interface, rather than in isolation. Accordingly, Fullston et al. [30,33] demonstrated that variations in zeta potential with pH under oxidizing conditions alter the surface charge density and, consequently, collector adsorption.

Microelectrokinetic and microflotation studies conducted by Castro and Honores [35] and Castro and Baltierra [38] demonstrated that enargite maintains a negative zeta potential across the entire evaluated pH range (2.5–12.0), with no defined isoelectric point. This behavior suggests that changes in zeta potential arise more from surface chemistry induced by oxidation and species adsorption than from a net charge neutralization associated with pH. Thus, the role of collectors becomes particularly relevant. Plackowski et al. [39] demonstrated that the adsorption of collectors such as sodium ethyl xanthate (SEX) and sodium dialkyl dithiophosphinate (3418A) on enargite occurs only under high electrochemical potential conditions (516 mV/SHE). In contrast, no adsorption evidence was observed at lower potentials (400 Mv/SHE), directly correlating with the recoveries obtained in microflotation. This behavior suggests that collectors not only adsorb onto active sites created by oxidation but also reinforce the negative surface charge, thereby modulating the zeta potential and, consequently, the hydrophobicity of the mineral.

Taken together, these investigations demonstrate that the zeta potential of enargite results from a complex balance between oxidation products, dissolved species, and reagent adsorption, rather than from an intrinsic electrokinetic parameter. Therefore, researchers should interpret zeta potential as an indirect indicator of the surface chemical state and its interaction with reagents, rather than as an independent property capable of predicting flotation response on its own.

2.3. Effect of Electrochemical Potential on the Enargite Surface Properties

Enargite has been the focus of numerous electrochemical studies due to its significance in the mining industry, particularly in copper ores processing and arsenic management. In this context, advanced analytical techniques including cyclic voltammetry (CV), X-ray Photoelectron Spectroscopy (XPS), scanning electron microscopy (SEM), energy-dispersive

X-ray spectroscopy (EDX), Raman spectroscopy (RS), synchrotron-based X-ray absorption near-edge structure (XANES), chronopotentiometry (CP), and electrochemical impedance spectroscopy (EIS) have been employed to gain deeper insight into the electrochemical behavior and surface transformations of enargite under varying physicochemical conditions.

Pauporté and Schuhmann [40] applied EIS, CV and photoelectrochemical experiments to investigate the enargite behavior under varying electrochemical potential. These authors showed that within the potential range of the flotation process (~240 mV/SHE) and at pH 9.3, a surface layer develops through two distinct stages, i.e., an initial phase characterized by the emergence of surface copper, followed by a subsequent phase involving the formation of soluble species. These findings were also reported by Córdoba et al. [5] who studied the electrochemical behavior of enargite in both stirred and stagnant aqueous solutions using alternating and direct current electrochemical techniques. These authors proposed that the release of copper ions predominates in the first stage of enargite oxidation, and that arsenic and sulfur containing species remain within the mineral structure. Furthermore, the authors identified that under reducing potential and at pH 4.6, electrode reactions during an anodic potential sweep, from −679 mV/SHE to −390 mV/SHE, lead to electro-oxidation as described in Equation (3).

$$2As + 3H_2S \rightarrow As_2S_3 + 6H^+ + 6e^- \quad (3)$$

In the pH range of 6.8 to 11.0, where species predominate, linear changes were observed between potential and pH, as shown in Equation (4):

$$2As + 3HS^- \rightarrow As_2S_3 + 3H^+ + 6e^- \quad (4)$$

Córdoba et al. [5] proposed that formation of arsenic trisulfide (As_2S_3) on the mineral surface plays a key role in the progressive development of a surface film that influences the reactivity of enargite and its capacity to adsorb flotation reagents. Ma et al. [41] using spectroscopic analysis such as cryo-stage XPS, RS, and XANES spectroscopy to demonstrate that enargite exhibits a passivation region between 647 and 947 mV/SHE related to the formation of an arsenic sulfide surface layer ($As_{(1-y-z)}S_4$).

Ma et al. [41] further proposed the existence of a trans-passive region between 947 and 1097 mV/SHE, associated with the partial dissolution of the passive film due to the oxidation of sulfur to elemental sulfur. Furthermore, copper preferentially dissolved over arsenic in the passive and trans-passive regions. Above 1097 mV/SHE, the passive film completely dissolved, generating elemental sulfur, as confirmed by RS and XANES studies.

In the initial study by Velásquez et al. [19], various oxidation and reduction potentials were applied to an enargite electrode using cyclic voltammetry (CV), followed by XPS analysis to determine the resulting surface composition. These authors showed that at potentials ~740 mV/SHE and at pH 9.2, the electrode surface is fully oxidized, forming compounds such as CuO, $CuSO_4$, and As_2O_x (x = 3; 5), in addition to copper hydroxides and polysulfides. The loss of copper on the surface and the reduction of Cu to Cu^+ at lower potentials indicated that the oxidized species remain stable only under elevated oxidation conditions. In a complementary study, Velásquez et al. [18] employed SEM, EDX, and EIS to investigate the morphological and electrochemical changes in the electrode under similar conditions. The results showed an irregular morphology and increased charge transfer at 740 mV/SHE, which was attributed to the formation of an oxidized layer on the surface. Both studies agreed that the oxidized layer, composed of CuO, As_2O_5, $CuSO_4$, and their hydroxides, significantly alters the surface conductivity and properties, highlighting the relationship between the applied potential and the stability of the oxidized species.

Ásbjörnsson et al. [42] studied the understanding of the oxidation and reduction mechanisms of the enargite surface in a 0.1 M HCl solution using techniques such as CV, CP, and EIS complemented by XPS and in situ RS. These authors reported that surface Cu^{2+} associated with sulfate can be detected at anodic potentials above 440 mV/SHE, indicating significant copper oxidation within this potential range. This study showed that arsenic oxidation occurred at around 840 mV/SHE with formation of minor amounts of As^{3+} and As^{5+} oxides at higher potentials. Dissolved arsenic in solution remained negligible in this study indicating rapid dispersion and possible reabsorption on the electrode surface. An active-passive transition was noted around 540 mV/SHE, while at 840 mV/SHE, sulfur concentration dropped. This behavior was attributed to the formation of an elemental sulfur layer that acts as a passivating barrier, preventing further oxidation of the enargite surface.

Guo and Yen [43] studied the electrochemical behavior of enargite under varying experimental conditions. These authors reported that $Cu(OH)_2$ is formed at potentials below 570 mV/SHE under neutral to alkaline pH, while Cu_2O and elemental sulfur are formed at higher oxidation conditions. Additionally, their studies did not detect $CuSO_4$ formation which differed with results obtained by other researchers who reported that $CuSO_4$ and $Cu(OH)_2$ can be formed though only at potentials above 740 mV/SHE. Furthermore, it was found that oxygen has no significant impact on the enargite's electrochemical behavior which disagrees with the observations by Ásbjörnsson et al. [42].

Lattanzi et al. [44] confirmed that significant surface changes occur only at high potentials (>740 mV/SHE) showing that at acidic pH values, the dominant process is copper dissolution, accompanied by the formation of elemental sulfur at 560 mV/SHE and pH = 1. These authors showed that several surface products can be formed at alkaline pH values including copper and arsenic oxides, and copper arsenates. Their XPS measurements confirmed the evolution of copper from the monovalent to the divalent state, formation of As-O bonds, and oxidation of sulfur to polysulfide, sulfite, and eventually sulfate.

Sasaki et al. [45] used XPS to study enargite oxidation under different pH conditions (2, 5, and 11), and in the presence of hydrogen peroxide (H_2O_2) and oxygen (O_2). Their results indicated that elemental sulfur forms on the enargite surface at pH 2.0 (Equation (5)) suggesting oxidative dissolution under acidic conditions. The authors showed that at pH 5.0 partial oxidation of arsenic from the enargite surface is observed leading to formation of $Cu_3(AsO_4)_2$ which is consistent with the proposed by Castro and Baltierra [38]. In contrast, at pH 11.0, enargite displayed more stability and lower susceptibility to oxidation compared to chalcopyrite and tennantite, with no formation of $Cu_3(AsO_4)_2$ due to the higher stability of $Cu(OH)_2$ under these conditions. This finding differs with the observations by Cordova et al. [5] who confirmed $Cu_3(AsO_4)_2$ formation through CV measurements. These authors also reported that on the unoxidized enargite surface the Cu^+ state dominates, with evidence of Cu^{2+} only at pH > 5.0 likely in the hydroxide form given the relatively higher solubility of copper oxides and sulfates [46].

$$2Cu_3AsS_4 + 11H_2O_2 + 10H^+ = 6Cu^{2+} + 2H_2AsO_4{}^- + 14H_2O + 8S \quad (5)$$

Plackowski et al. [47] studied the surface properties of natural enargite in a 0.05 M buffer solution at pH 10.0 (sodium tetraborate decahydrate and sodium hydroxide), and in a 0.1 M buffer solution at pH 4.0 (glacial acetic acid and sodium acetate). The authors described that the anodic peaks in Figure 6, generated by cyclic polarization of enargite at pH 10.0, represent a process of progressive copper dissolution from the mineral surface to the Cu^{2+} form, along with arsenic oxides, elemental sulfur, and sulfates. Peaks 1 to 5 can be associated with chemical reactions observed during the anodic scan, ranging from weak oxidation (Equation (6)) to complete mineral dissolution (Equation (10)), with intermediate

reactions showing elemental sulfur formation. These authors corroborated the results obtained by Guo and Yen [43], Velasquez et al. [19], and Cordova et al. [5].

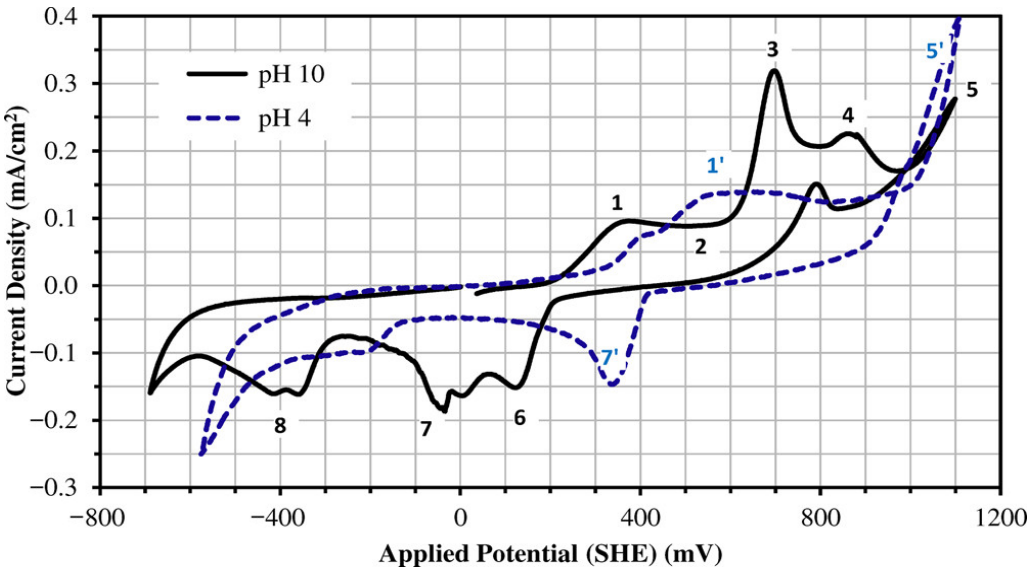

Figure 6. Typical cyclic voltammograms for natural enargite at pH 10 (solid black line) and pH 4 (dashed blue line) obtained using a scan rate of 1 mV/s (ref. [47] with permission).

For the anodic scan, the reactions proposed are displayed in Equations (6)–(10).

$$Cu_3AsS_4 + 2xOH^- = Cu_{3-x}AsS_4 + xCu(OH)_2 + 2xe^- \quad (6)$$

$$Cu_{3-x}AsS_4 + (14-2x)OH^- = (3-x)Cu(OH)_2 + AsO_4{}^{3-} + 4S^0 + 4H_2O + (11-2x)e^- \quad (7)$$

$$Cu_2AsS_4 + 12OH^- = 2Cu(OH)_2 + AsO_4{}^{3-} + 4S^0 + 4H_2O + 9e^- \quad (8)$$

$$CuAsS_4 + 10OH^- = Cu(OH)_2 + AsO_4{}^{3-} + 4S^0 + 4H_2O + 7e^- \quad (9)$$

$$Cu_3AsS_4 + 46OH^- = 3Cu(OH)_2 + AsO_4{}^{3-} + 4SO_4{}^{2-} + 20H_2O + 35e^- \quad (10)$$

For the cathodic scan, the reactions proposed are displayed in Equations (11)–(14).

$$2Cu(OH)_2 + 2e^- = Cu_2O + 2OH^- + H_2O \quad (11)$$

$$2S^0 + 2e^- = S_2{}^{2-} \quad (12)$$

$$S_2{}^{2-} + 2e^- = 2S^{2-} \quad (13)$$

$$2Cu_3AsS_4 + 6H_2O + 6e^- = As_2S_2 + 3Cu_2S + 3H_2S + 6OH^- \quad (14)$$

Plackowski et al. [37] quantified the chemical changes on the enargite surface at five anodic potentials that were identified by CV studies to be significant to characterize the progression of induced chemical transformations, i.e., 347, 516, 705, 869 and 1100 mV/SHE. The results showed that between 347 and 516 mV/SHE, copper dissolution was observed, which led to a copper-deficient surface without evidence of Cu^{2+} species such as hydroxides or sulfates, which disagrees with the findings by Guo and Yen [43]. Additionally, it was concluded that an initial oxidation peak observed at 288 mV/SHE leads to copper oxidation to Cu^{2+} which precipitates as $Cu(OH)_2$ on the enargite surface. The presence of sulfate ($SO_4{}^{2-}$) was detected above 516 mV/SHE and persisted at higher potentials while $CuSO_4$ only appeared from 705 mV/SHE onward, alongside with $Cu(OH)_2$ and CuS, though CuS replaced $Cu(OH)_2$ at higher potentials. The XPS and thermodynamic data confirmed these species, along with arsenic oxides, likely As_2O_3. Photoelectron spectra indicated a

decrease in Cu and As on the surface above 705 mV/SHE, supporting the hypothesis of progressive Cu and As dissolution, with a layer of sulfates, CuS, and As_2O_3 forming at higher potentials.

García-Garnica et al. [48] investigated the oxidation of enargite at alkaline conditions using different oxidizing agents, i.e., H_2O_2, sodium hypochlorite (NaClO), calcium hypochlorite ($Ca(ClO)_2$), and potassium permanganate ($KMnO_4$). CV and EIS techniques were employed to assess the oxidation response of the mineral. The voltammetric response of an enargite electrode at pH 10.0 was evaluated at different scan rates within a potential window of −440 to 600 mV/SHE, revealing two oxidation processes (AE1 and AE2) and two reduction processes (CE1 and CE2) as shown in Figure 7.

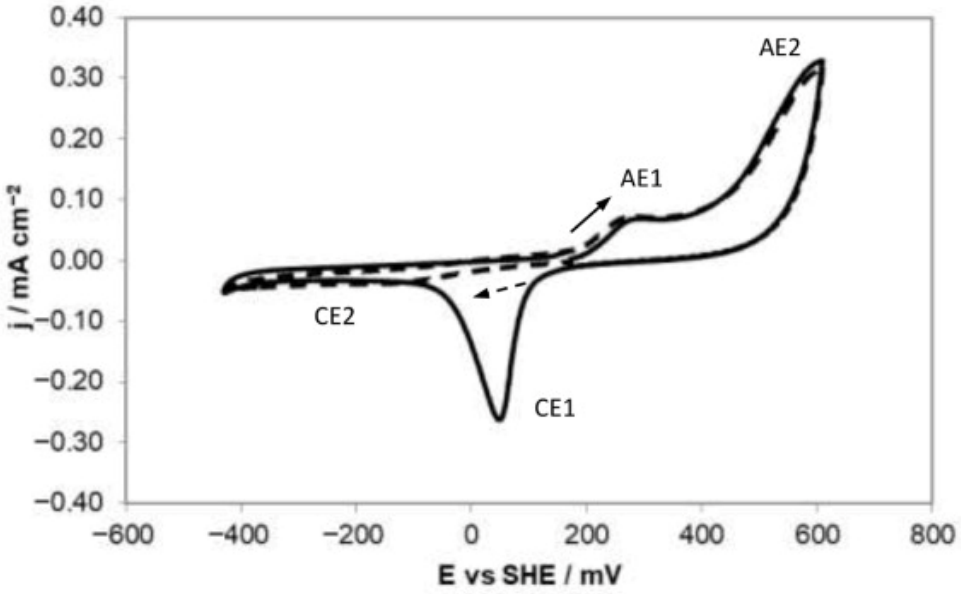

Figure 7. Comparison of the electrochemical behavior obtained when the initial scan is performed in the positive direction (—) and in the negative direction (- - -) for a natural enargite electrode in a buffered solution at pH 10 and a scan rate of 5 mV/s (ref. [48] with permission).

By comparing cyclic voltammograms of enargite with scans in positive and negative directions to differentiate surface reduction processes on the mineral from oxidation products, it was determined that the AE1 peak, observed at 290 mV/SHE, corresponds to the initial oxidation of enargite and is associated with a passive process. Meanwhile, AE2, which appears at potentials above 400 mV/SHE, represents a transpassive zone. The behavior of AE1 aligns with previous studies by Guo and Yen [43] which are summarized in Equation (15), though differences in potential were noted depending on the experimental method and impurities in the mineral electrode [47].

$$Cu_3AsS_4 + 2xOH^- \rightarrow Cu_{3-x}AsS_4 + xCu(OH)_2 + 2xe^- \quad (15)$$

The results and mechanisms proposed by García-Garnica et al. [48] indicate that at potentials below 400 mV, partial oxidation occurs on the enargite surface, resulting in the progressive dissolution of Cu^+ which subsequently oxidizes to Cu^{2+}. At pH 10.0, Cu^{2+} precipitates as $Cu(OH)_2$, potentially explaining the observed current plateau. However, the results of XPS analysis by Plackowski et al. [37] questions the formation of $Cu(OH)_2$ at this potential, citing the absence of a Cu^{2+} signal, although the authors acknowledge the possible presence of Cu^{2+} ions in the surrounding solution. García-Garnica et al. [48] studied the voltammetric response of enargite under different agitation conditions and by adding ethylenediaminetetraacetic acid (EDTA) to sequester Cu^{2+} ions. Figure 8 compares

the enargite voltammograms at 0 and 300 rpm, showing a decrease in current at the CE1 peak, which suggests its association with the reduction products of AE1 and AE2 from Figure 7, and thus labeled as CE1′. Therefore, the similar voltametric response of AE1 and CE1′ with and without rotation confirms the formation of insoluble products in AE1, which are subsequently reduced in CE1′. The addition of EDTA altered the AE1 plateau and removed the CE1′ reduction process. This effect is attributed to forming a Cu^{2+}-EDTA complex that diffuses from the surface into the solution volume. Thus, these results support the formation of $Cu(OH)_2$ in AE1.

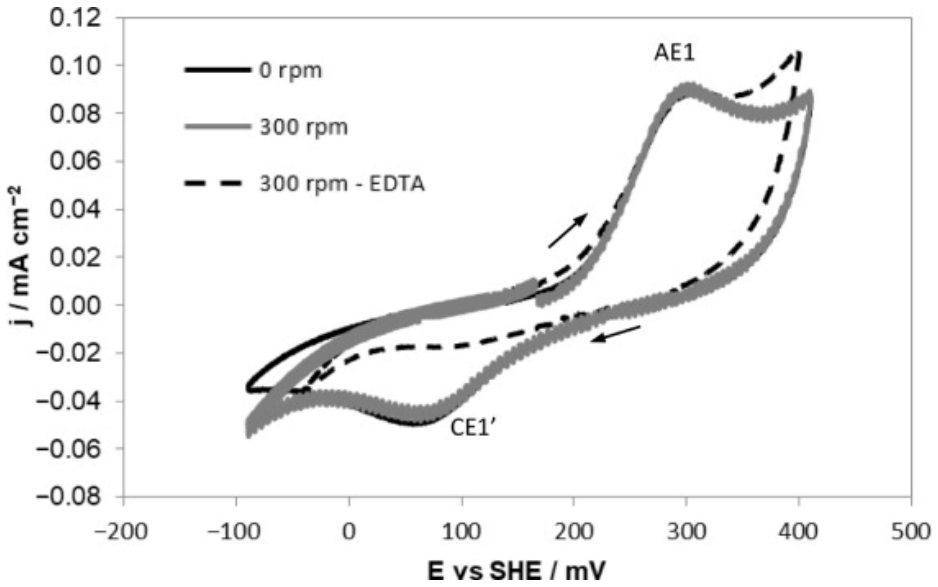

Figure 8. Effect of rotation and EDTA addition on the electrochemical behavior of a natural enargite electrode in a buffered solution at pH 10 with a scan rate of 5 mV/s (ref. [48] with permission).

Plackowski et al. [37,39] and Gow et al. [49] propose that the oxidation of enargite at pH 10.0 in the potential range from 200 to 1000 mV/SHE can be described by Equation (16). This supports the suggestion of a progressive dissolution of enargite until reaching an overpotential that facilitates complete oxidation.

$$Cu_3AsS_4 + 26H_2O \rightarrow 3Cu(OH)_2 + HAsO_4{}^{2-} + 4SO_4{}^{2-} + 45H^+ + 35e^- \quad (16)$$

It was proposed that CE1 corresponded to the reduction in oxidation products, including both $Cu(OH)_2$ and $HAsO_4{}^{2-}$ (referred to hereafter as As^{5+}), as described in Equations (17) and (18).

$$2Cu(OH)_2 + 2e^- \rightarrow Cu_2O + 2OH^- + H_2O \quad (17)$$

$$HAsO_4{}^{2-} + 2e^- + 2H^+ \rightarrow HAsO_3{}^{2-} + H_2O \quad (18)$$

It was also proposed that the initial oxidation at AE1 (Figure 8) at potentials below 400 mV/SHE relates to $Cu(OH)_2$ formation, and that the oxidation processes between 400 and 600 mV/SHE release soluble arsenic and generate polysulfides, which oxidize to sulfate, aligning with other studies [37,39,44].

2.4. Contact Angle

In froth flotation, the contact angle is a key parameter for evaluating the wettability of mineral surfaces, which directly affects their floatability. This parameter corresponds to the angle (measured through the liquid phase) formed by the tangent to a water droplet at the

point where the solid, liquid, and gas phases meet (the triple point) and the solid–liquid interface. At equilibrium, this angle is governed by the laws of thermodynamics and depends on the balance of surface energies among the different phases. A high contact angle indicates a hydrophobic surface, while a low contact angle means a hydrophilic surface, where water spreads readily and the particle tends to remain in the pulp phase. This measurement is essential for assessing the effectiveness of flotation reagents and has been used to assess the floatability of metal sulfides such as enargite.

Guo and Yen [50] studied the surface hydrophobicity of enargite in potassium amyl xanthate (PAX) solutions by taking contact angle measurements and conducting electrochemical studies. Their results indicated that enargite became hydrophobic at 40 mV/SHE and pH 10.0, exhibiting a contact angle of 90° within the potential range between 91 and 1090 mV/SHE. At pH 7.0, hydrophobicity was observed to begin at −34 mV/SHE, with a contact angle of 90° achieved within the same range. These authors also investigated the effect of PAX concentration on the floatable potential range of enargite and its relationship with the contact angle. They found that the contact angle in a 7×10^{-5} M PAX solution was approximately 10° lower than that in a 7×10^{-4} M PAX solution. This difference was attributed to the increased surface oxidation of enargite at higher potentials in the more dilute solution [51]. In contrast, in the more concentrated solution, xanthate ions inhibited oxidation, maintaining a higher contact angle.

Guo and Yen [8] used contact angle measurements and electrochemical polarization studies to compare the selective floatability of enargite and chalcopyrite in 7×10^{-4} and 7×10^{-5} M PAX solutions, and at pH 10.0 (Figures 9 and 10). Their results reported in Figure 9 showed that at a PAX concentration of 7×10^{-4} M, the contact angle on the natural enargite surface remained stable over a potential range between 141 and 1081 mV/SHE while the contact angles of chalcopyrite are slightly lower across the studied potential range. In contrast, the results in the 7×10^{-5} M PAX solution (7×10^{-5} M) shown in Figure 10 reveal significant differences in hydrophobicity between enargite and chalcopyrite with the contact angle of the latter being considerably lower than the former mineral, with this difference becoming more pronounced at potentials above 440 mV/SHE. These findings suggest that under oxidizing and alkaline conditions, a more efficient selective separation between these minerals could be achieved.

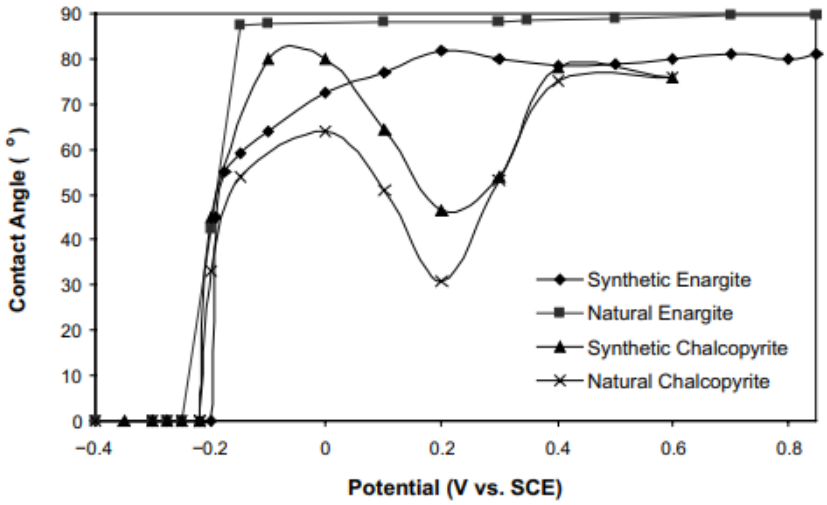

Figure 9. Contact angle of enargite and chalcopyrite in a 7×10^{-4} M PAX solution at pH 10 (ref. [8] with permission).

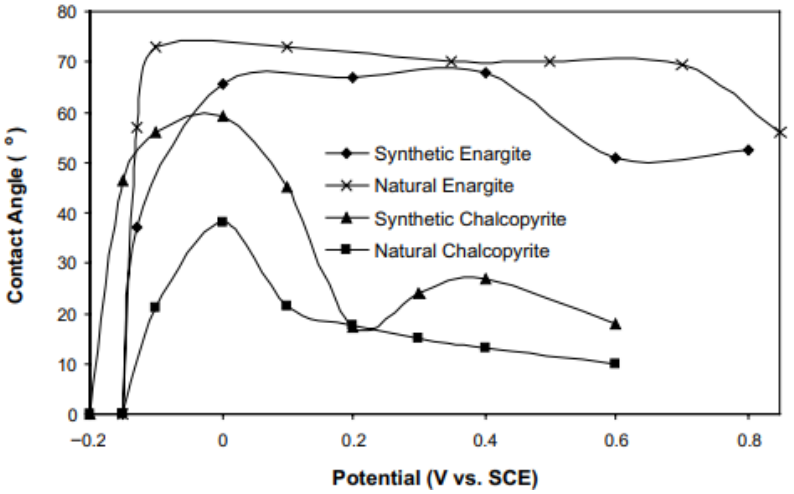

Figure 10. Contact angle of enargite and chalcopyrite in 7×10^{-5} M PAX solution at pH 10 (ref. [8] with permission).

Further studies on the hydrophobicity changes associated with surface oxidation of enargite were carried out by Plackowski et al. [47]. These authors conducted contact angle measurements on a freshly polished enargite surface subjected to three separate preparation conditions, i.e., a polished surface without additional treatment, a polished surface oxidized for 60 min at 610 mV and pH 4.0, and a polished surface oxidized for 60 min at 869 mV/SHE and pH 10.0. The results indicated that the initial contact angle for a freshly polished surface without additional treatment was 46.1 ± 3.5°; the contact angle for an oxidized surface at pH 4.0 was 59.1 ± 7.1°; and the contact angle on a surface oxidized at pH 10.0 was 44.4 ± 8.6°, showing considerable variation between 35.2 and 55.2°, suggesting a non-uniform oxidation layer.

Gan et al. [52] studied the flotation separation of enargite and covellite by analyzing the hydrophobicity of the mineral surfaces after oxidation treatment with NaClO and ferric chloride ($FeCl_3$). Their results showed that, after treatment with ammonium dibutyl dithiophosphate (ADD), the contact angles were 96.7° for covellite and 92.6° for enargite, indicating high hydrophobicity on both surfaces. The application of NaClO and $FeCl_3$ led to a decrease in contact angles, with a more pronounced reduction observed using $FeCl_3$, suggesting a more significant variation in surface hydrophobicity. Additionally, the differences in the contact angles of covellite and enargite increased from 4.1° to −14.2°, indicating that the oxidizing agents enhance the disparity in hydrophobicity between the two surfaces, aligning with flotation test results.

It is important to note that while the contact angle is a key parameter for evaluating the hydrophobicity of a mineral surface, its isolated interpretation is limited in fully understanding the interaction between the mineral and the collector in a flotation system, as multiple variables can influence the measurements and hinder the attainment of conclusive results [53]. Factors such as surface roughness, chemical heterogeneity, the presence of micro- and nanostructures, and the hydrodynamic conditions during sample preparation can significantly alter the apparent contact angle, generating amplification or masking effects that complicate its subsequent analysis [53,54]. The interaction or overlap of these factors in each analyzed system makes it difficult to differentiate their individual effects, preventing the establishment of a universal correlation between the contact angle and flotation recovery based on fundamental principles. Moreover, variability in surface chemical composition influences collector adsorption, directly affecting mineral floatability. Therefore, for a more precise characterization of hydrophobicity, it is essential to complement contact angle analysis with other techniques.

3. Flotation of Enargite

As discussed in Chapter 1, the separation of enargite from other copper sulfide minerals by flotation presents a significant challenge due to the similarities in their surface properties, flotation responses, and reagent adsorption behavior [55]. Enargite, a copper arsenic mineral, often exhibits flotation characteristics that closely resemble those of primary and secondary copper sulfides such as chalcopyrite, bornite, and chalcocite. This makes selective separation difficult using conventional reagents and conditions. To address this issue, various approaches have been explored, including the use of selective depressants and collectors designed to differentiate enargite from other sulfide minerals. Additionally, controlling the pulp electrochemical potential has been shown to influence mineral surface chemistry and enhance selectivity. The application of specific reagents that promote selective surface oxidation of enargite has also been investigated as a means to suppress its flotation while allowing other sulfides to float. Furthermore, the increasing use of seawater in flotation processes-driven by freshwater scarcity in mining regions-adds another layer of complexity to the separation process. The high ionic strength and presence of divalent cations in seawater can significantly affect reagent performance, mineral surface interactions, and ultimately, flotation selectivity. Therefore, the impact of seawater chemistry must also be carefully considered in any comprehensive analysis of enargite separation strategies.

3.1. Selective Flotation Reagents

In selecting suitable reagents for the selective separation of arsenic-bearing minerals from copper sulfides, various compounds with potential applicability have been investigated. One of the most studied reagents to achieve this objective is the magnesium-ammonium mixture (MAA) which has been used as enargite depressant. Tajadod and Yen [56] studied and compared the use of MAA, sodium sulfide (Na_2S), and pulp aeration as conditioning methods. Their results indicated that MAA conditioning was the most effective, significantly reducing xanthate adsorption on enargite and enabling the separation of the arsenic-bearing minerals without compromising chalcopyrite floatability. Enargite recovery was reduced from 71 to 15%, while chalcopyrite recovery slightly decreased from 81 to 80%. When aeration was combined with MAA, recoveries further decreased to 12% for enargite and 79% for chalcopyrite. The authors concluded that MAA effectively promotes the flotation separation of enargite from chalcopyrite by forming a stable, hydrophilic compound with arsenic on the enargite surface ($MgNH_4AsO_4 \cdot 6H_2O$) which inhibits xanthate adsorption on this mineral [57].

Yen and Tajadod [58] further investigated the selective flotation of chalcopyrite and enargite using MAA as a depressant while controlling the pulp potential. Their results demonstrated that at pH values between 7.0 and 9.0, and within the potential range between −145 and 14 mV/SHE for enargite, and −160 and 100 mV/SHE for chalcopyrite, enargite recovery was reduced to values below 15%, while chalcopyrite maintained a recovery of approximately 80%–82%. It was shown that pre-aeration prior to MAA addition further decreased enargite recovery to 2.3% without affecting chalcopyrite, suggesting that selective flotation of enargite from chalcopyrite can be effectively achieved through pulp potential control combined with the use of MAA as a depressant. Castro et al. [59] investigated the effect of MAA on enargite during the cleaning stage of a copper ore flotation, within a pH range between 7 and 10, and using MAA dosages between 1.8 and 10.8 kg/t. Their results showed that the depressing effect of MAA was limited, which differed from the findings by Yen and Tajadod [58]. Castro et al. [59] proposed that the absence of a pre-aeration stage could explain the limited effectiveness of MAA under their conditions, highlighting the importance of this step in optimizing the depressant effect during flotation. Yen and

Tajadod [58] and Dai et al. [60] implemented pre-aeration properly, demonstrating that it is crucial for effective enargite depression. It is important to mention that these inconsistencies highlight the importance of simultaneously considering multiple factors, including mineral surface morphology, electrochemical behavior, pulp pH, and collector effects, all of which determine the selectivity of flotation processes.

The previously described studies on the use of MAA in the selective flotation of enargite and copper sulfides suggested that the depressing effect of this reagent arises from the formation of $MgNH_4AsO_4 \cdot 6H_2O$, and that pH plays a critical role in this mechanism. However, Pineda et al. [6], who investigated the influence of pH on the adsorption of magnesium compounds on the enargite surface using XPS and cyclic voltammetry, reported findings that challenge this proposed mechanism. They showed that at pH 12.0, $Mg(OH)_2$ precipitation occurs, while no precipitation was observed at pH 10.0. Furthermore, pre-oxidation did not promote the precipitation of magnesium compounds at any of the pH levels analyzed, and the formation of $MgNH_4AsO_4 \cdot 6H_2O$ was not detected under any of the tested conditions.

Alternatively, the use of MAA as a depressant has been explored for other arsenic-bearing minerals. Tapley and Yan [61] investigated its effect on arsenopyrite depression, identifying the optimal conditions to improve its separation from pyrite. The results showed that MAA addition significantly reduced the floatability of arsenopyrite without considerably affecting pyrite. This effect was achieved with an MAA concentration of 250 mg/L at pH 8.0, combined with 2.14×10^{-3} mol/L of sodium ethyl xanthate (SEX) as a collector.

Potassium permanganate ($KMnO_4$), sodium cyanide (NaCN), and Na_2S have also been evaluated for the selective separation of enargite and copper sulfides but with limited success. Tajadod and Yen [62] investigated the selective flotation of enargite and chalcopyrite using NaCN and $KMnO_4$ as depressants. They found that both reagents reduced xanthate adsorption on enargite but the use of NaCN achieved only partial arsenic separation (70% arsenic rejection) at the cost of 45% of copper losses rendering the process industrially unfeasible. The presence of copper ions on the surfaces of enargite and copper sulfides facilitates the formation of soluble cyanide complexes, such as $[Cu(CN)_2]^-$ leading to progressive copper dissolution. Although this cyanide action promotes enargite depression and reduces arsenic content, it also causes significant copper losses from other copper sulfides. Moreover, pre-conditioning with NaCN followed by xanthate addition further decreases the final xanthate adsorption density on both minerals, directly affecting their surface hydrophobicity. Similar results were observed using $KMnO_4$ as depressant for the selective flotation of enargite from other sulfides. Additionally, Tajadod [63] expanded the research on selective flotation techniques by comparing the previously studied performance of NaCN and $KMnO_4$ with that of Na_2S, aiming to optimize the separation of enargite and chalcopyrite in a synthetic copper concentrate. The results showed that NaCN, at a concentration of 20 mg/L and a contact time of 20 min, provided the highest efficiency as a depressant for copper/arsenic separation, achieving a copper recovery of 55.2% and the lowest arsenic content in the concentrate, consistent with the findings of Tajadod and Yen [62].

Suyantara et al. [64] investigated the impact of sodium sulfite (Na_2SO_3) on the floatability of enargite and chalcopyrite through microflotation tests conducted on both individual and mixed mineral systems. These tests were complemented with XPS surface analysis to explain the observed phenomena. The results, presented in Figure 11, showed that in individual mineral systems, the addition of Na_2SO_3 depressed the floatability of both minerals at pH 9.0 in the absence of PAX. However, when 0.1 mM PAX was added prior to Na_2SO_3, a slight reduction in enargite recovery was observed, while chalcopyrite recovery

significantly decreased at Na_2SO_3 concentrations above 1.0 mM. These flotation results suggest that the selective separation of enargite and chalcopyrite could be achieved by adding Na_2SO_3 in the presence of PAX.

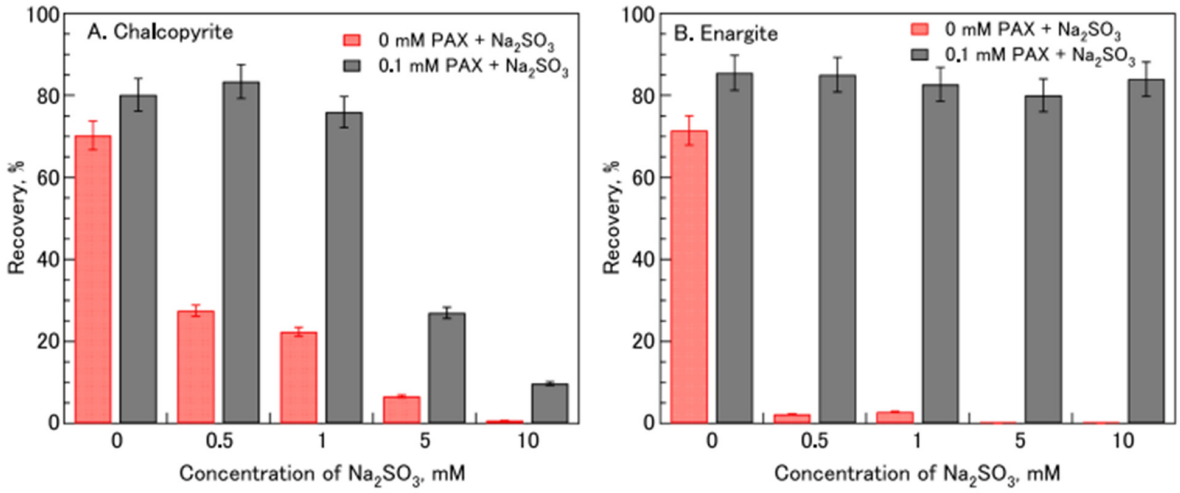

Figure 11. Effect of Na_2SO_3 on chalcopyrite and enargite recovery in individual mineral systems at pH 9, both in the absence and presence of PAX (ref. [64] with permission).

To better analyze their results in mixed mineral systems (Figure 12), Suyantara et al. [64] proposed the use of the Newton efficiency defined in Equation (19). In the absence of PAX (Figure 12A), their results showed that Na_2SO_3 generated a depressing effect on the floatability of both enargite and chalcopyrite which became more pronounced at higher reagent concentrations. The low Newton efficiency values shown in Figure 12A suggest that achieving selective separation of the two minerals using Na_2SO_3 alone is challenging.

$$Newton\ efficiency = Recovery\ of\ enargite - Recovery\ of\ chalcopyrite \quad (19)$$

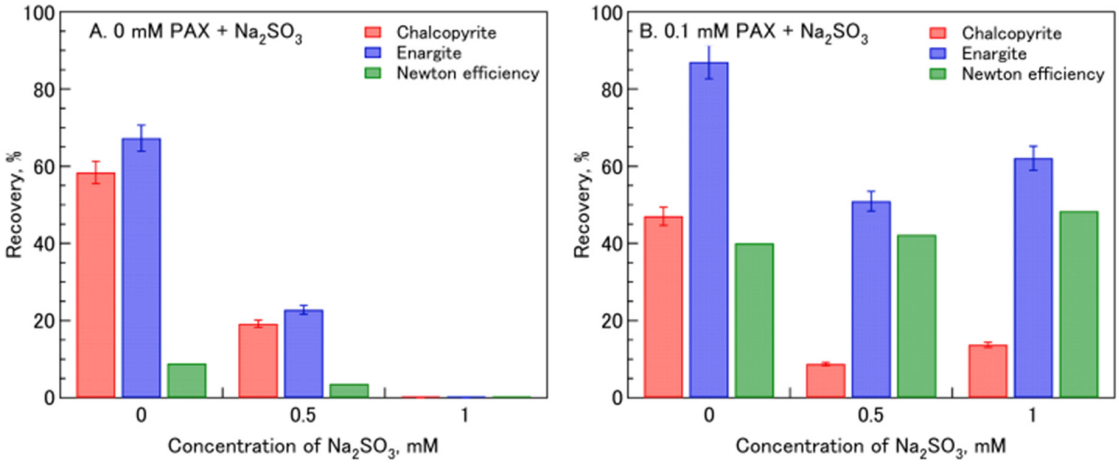

Figure 12. Effect of Na_2SO_3 on chalcopyrite and enargite recovery in a mixed mineral system at pH 9 in the presence of PAX (ref. [64] with permission).

Figure 12B shows the results obtained by Suyantara et al. [64] in the presence of 0.1 mM PAX at different Na_2SO_3 dosages. The data indicate that the addition of Na_2SO_3 reduced the recovery of both enargite and chalcopyrite, with a stronger depressing effect observed on chalcopyrite. A Newton efficiency of 48% was achieved after treatment with 0.1 mM PAX and 1.0 mM Na_2SO_3, suggesting that chalcopyrite floatability can be effectively depressed while maintaining the floatability of enargite. It is interesting to analyze the results obtained

by Suyantara et al. [64] in the presence of PAX and at a Na_2SO_3 concentration of 0 mM. It can be observed that chalcopyrite recovery decreases compared to tests without PAX, while enargite recovery increases. This behavior differs from previous flotation studies with individual minerals, suggesting a possible interaction between chalcopyrite and enargite that affects PAX adsorption on both mineral surfaces. Suyantara et al. [64] proposed that this interaction promotes the predominant formation of CuS on the enargite surface, enhancing its floatability, while chalcopyrite surfaces develop FeOOH, FeS_2, Fe_2 $(SO_4)_3$, and sulfate species, which reduce its floatability. Additionally, adding Na_2SO_3 after PAX treatment reduces the proportion of CuS on both surfaces and promotes the formation of sulfate species on chalcopyrite, further depressing its flotation and improving enargite recovery. Previous studies have reported this disparity [8,65]. Guo and Yen [8] suggested that these phenomena might involve galvanic interactions between chalcopyrite and enargite. However, further study is necessary to confirm this galvanic interaction.

Recent findings by Lin et al. [66] demonstrated that calcium lignosulfonate can act as an effective depressant for selective separation between covellite and enargite. Using contact angle measurements, adsorption tests, SEM–EDS and XPS analyses, the authors elucidated that the reagent exhibits differential adsorption on the two mineral surfaces, which results in distinct flotation behaviors. Pure mineral flotation tests showed that calcium lignosulfonate enabled the production of separate copper concentrates from artificially mixed ores: a low-arsenic concentrate (Cu 55.36%, As 4.98%) and a high-arsenic concentrate (Cu 52.74%, As 10.46%). Furthermore, bench-scale flotation tests confirmed that combining reagent removal via activated carbon, pH adjustment with CaO, and selective depression with calcium lignosulfonate yielded a low-arsenic copper concentrate (As 0.57%) alongside an arsenic-rich fraction. The study concluded that selective depression is primarily governed by the stronger adsorption of calcium lignosulfonate onto enargite surfaces compared to covellite, thereby enhancing arsenic separation efficiency during flotation.

Table 1 shows a summary of the different studies on the use of reagents in the selective flotation of enargite from other sulfides.

Table 1. Summary of different studies on the use of reagents in the selective flotation of enargite.

Source	Reagents	Main Findings
[62]	NaCN, $KMnO_4$	NaCN and $KMnO_4$ depress enargite and chalcopyrite but cause significant copper losses (45%).
[56]	Na_2S, MAA	MAA allows the separation of 50% of the arsenic without affecting the buoyancy of the chalcopyrite.
[63]	NaCN, $KMnO_4$, Na_2S	NaCN achieved the best Cu-As separation with 55.2% Cu recovery and minimal As content. $KMnO_4$ and Na_2S were less effective.
[58]	MAA	MAA reduces xanthate adsorption on enargite without affecting chalcopyrite. Pre-aeration improves selective flotation.
[59]	MAA	At pH 10.0 with 2.5 kg/t MAA, 55% recovery is obtained. Higher doses reduce the depressive effect of MAA.
[6]	MAA	The formation of $MgNH_4AsO_4$-$6H_2O$ was not observed. In addition, Mg has no passivating effect under alkaline conditions.
[64]	Na_2SO_3, PAX	Na_2SO_3 enhances the selective flotation of enargite in the presence of PAX, while depressing chalcopyrite in mixed systems.
[66]	Ca-lignosulfonate, CaO, activated carbon	Differential adsorption of Ca-lignosulfonate on enargite surfaces selectively depresses enargite over covellite. Bench-scale tests combining reagent removal with activated carbon, pH adjustment using CaO, and Ca-lignosulfonate depression produced low-As copper concentrates (As 0.57%) and arsenic-rich fractions.

3.2. Pulp Potential and pH Control

The control of pulp electrochemical potential and pH has previously been proposed as a strategy to achieve selective separation between enargite and other copper sulfide minerals [5,8,67–71]. By adjusting these parameters, it is possible to influence the surface oxidation states and mineral-reagent interactions, thereby modifying the flotation behavior of the respective minerals. Enargite, in particular, is known to respond differently to changes in redox potential compared to minerals such as chalcopyrite or chalcocite, which can be exploited to enhance separation efficiency. Additionally, pH plays a critical role in determining the speciation of flotation reagents and dissolved metal ions, which in turn affects surface charge, hydrophobicity, and adsorption dynamics. When optimized together, pulp potential and pH can create conditions under which the flotation of enargite is suppressed while promoting the recovery of other copper sulfides, making this approach a valuable tool in arsenic management and clean copper concentrate production.

Kantar [68] studied the flotation behavior of enargite using microflotation tests under varying electrochemical potentials controlled using H_2O_2 and Na_2S. The results at pH 2 under collectorless conditions indicate that enargite exhibits natural floatability under oxidizing conditions which decreases under reducing conditions. At pH values lower than 5.5, enargite becomes more hydrophobic as pulp potential increases which is explained by the formation of CuS and S^0 at the surface. These results agree with previous reported studies [5,67,69–71]. This author reported that at alkaline pH, enargite hydrophobicity decreases with the increase in pulp potential due to the formation of CuO, H_2AsO^{4-} and SO_4^{2-} compounds being the copper oxide the most relevant in making the enargite surface hydrophilic. Figure 13 presents the results obtained by Kantar [68] regarding enargite flotation recovery as a function of Eh, in the presence of the collector sodium ethyl xanthate (NaEX) at a concentration of 5×10^{-3} M and pH 10.5. The results show that enargite recovery reaches a maximum value close to 100% within an Eh range between 150 and 270 mV/SHE and decreases sharply at potentials outside this range. These findings suggest that enargite floatability is highly sensitive to pulp potential as its recovery peak falls within a narrow potential window and declines significantly outside it.

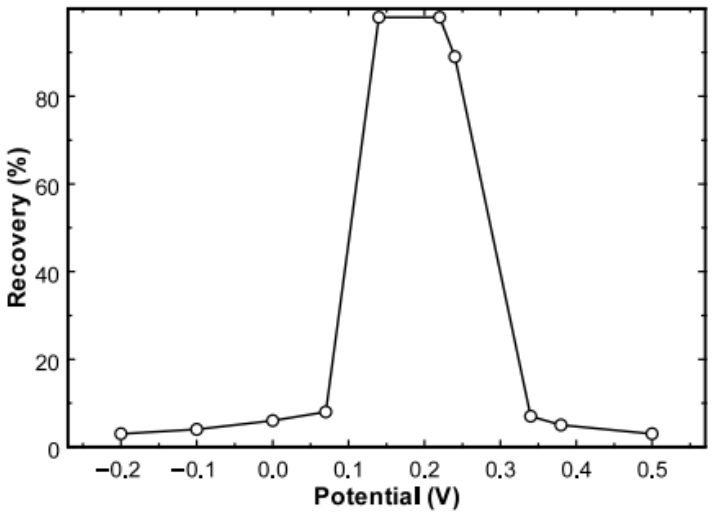

Figure 13. Enargite flotation recovery as a function of E_h in the presence of sodium ethyl xanthate (NaEX) at a concentration of 5×10^{-3} M, and at pH 10.5 (ref. [68] with permission).

Guo and Yen [8] investigated the flotation behavior of natural and laboratory-synthesized enargite and chalcopyrite samples. They conducted electrochemical studies, contact angle measurements, and microflotation tests, both with and without collectors, on

single-mineral and composite systems (comprising 50% synthetic enargite and 50% synthetic chalcopyrite). The results presented in Figure 14 for single-mineral systems showed that enargite recovery is higher than 90% in the pulp potential range between −100 and 450 mV/SCE (standard calomel electrode), but it sharply decreases outside this range. Enargite's floatability sharply decreases above 450 mV/SCE, indicating the formation of a passivating oxidation layer that hinders the flotation process most likely composed of compounds such as $Cu(OH)_2$ that act as hydrophilic barriers on the enargite surface. On the other hand, chalcopyrite recovery reaches values between 80 and 90% in the pulp potential range between −100 and 150 mV/SCE with a strong depression at higher Eh values. These results show that at a pH value of 10 and potentials greater than 150 mV/SCE, it may be possible to separate both minerals by flotation.

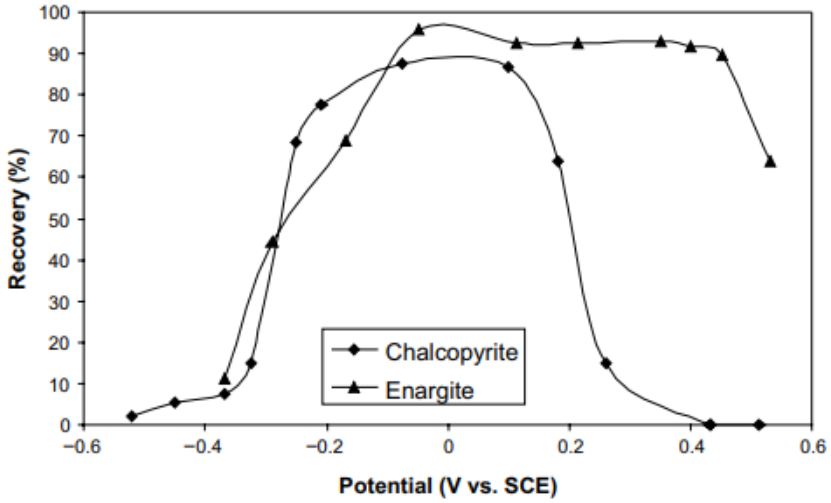

Figure 14. Single-mineral tests of the effect of pulp potential on the floatability of enargite and chalcopyrite in a 7×10^{-5} M PAX solution at pH 10 (ref. [8] with permission).

Figure 15 shows the results obtained by Guo and Yen [8] with a synthetic composite ore sample (mixed mineral system) containing enargite and chalcopyrite in a 7×10^{-5} M PAX solution at pH 10.0. The results show that at a potential of 200 mV/SCE the enargite recovery reaches values of 98% while chalcopyrite recovery was close to 21%. At higher pulp potentials, enargite recovery slightly decreased to values close to 93% at 500 mV/SCE while chalcopyrite recovery decreased to 7% at the same pulp potential. According to these data, the best separation between both minerals is achieved at 500 mV/SCE as indicated by the selectivity curve presented in Figure 15. Guo and Yen [8] reported better floatability of enargite in the synthetic composite ore compared to the single mineral-system which was explained by the galvanic interactions between enargite and chalcopyrite that enhance enargite stability during flotation. This hypothesis is supported by the results obtained by Suyantara et al. [64,65] who proposed that the formation of CuS on the enargite surface improves its floatability, although additional studies are required to confirm this mechanism. The influence of galvanic interactions in the enargite–copper sulfides system was also reported by other authors [72,73].

Subsequently, Guo and Yen [74] reported good flotation of enargite over a potential range of 190–740 mV/SHE in a PAX solution at 7×10^{-5} M, supporting their previous results for a single mineral system. These results differ from those reported by Kantar [68], who observed a narrower potential range of 150–270 mV/SHE. This discrepancy can be attributed to the different types of collectors used in the two studies as Guo and Yen [74] employed PAX whereas Kantar [68] used NaEtX. PAX, with its longer hydrocarbon chain

compared to NaEtX, enables more efficient adsorption onto the enargite surface over a wider range of potentials, thus broadening the potential window for flotation to occur.

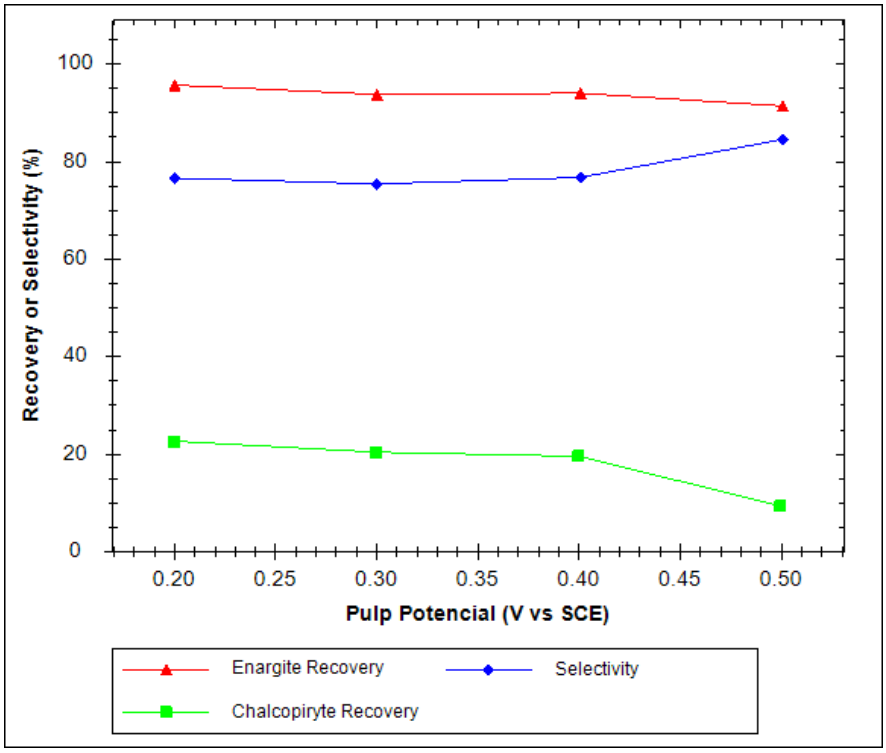

Figure 15. Mixed-mineral tests of the effect of pulp potential on the selective flotation of enargite and chalcopyrite in a 7×10^{-5} M PAX solution at pH 10 (Adapted from [8]).

Senior et al. [75] investigated the selective separation of enargite from other copper sulfide minerals using an artificial ore composed of 10% natural enargite and 90% quartz. These authors studied the flotation response over an Eh range between −500 and 500 mV/SHE at pH values of 8 and 11. Results from the single-mineral flotation tests showed that enargite floats at Eh values higher than −75 mV/SHE at pH 8, and higher than 25 mV/SHE at pH 11 which is in agreement with the results obtained by Guo and Yen [8]. The results from the mixed-mineral flotation tests obtained by Senior et al. [75] showed that the floatability of chalcopyrite, chalcocite, pyrite, and enargite is low under strongly reducing conditions (Eh < −200 mV/SHE) as seen in Figure 16. These authors also showed that enargite can be separated from chalcocite and chalcopyrite at 0 mV/SHE, and at either pH 8.0 or 11.0. Additionally, enargite can be floated from chalcocite and cuprite at pH 11.0 with a potential of 290 mV/SHE.

To further investigate the floatability of arsenic within copper minerals and optimize its separation, Bruckard et al. [76] conducted a study on the flotation of metallic arsenic using ethyl xanthate. Their research evaluated the effects of pH and pulp potential (Eh) in a synthetic mixture of metallic arsenic and quartz. The findings revealed that despite arsenic's lack of natural floatability, up to 95% recovery could be achieved across a broad range of pH and pulp potential values. Guo and Yen [43] complemented these findings by identifying the formation of a passivating layer over a wide potential range (−660 to 1070 mV/SHE). They observed that copper hydroxide ($Cu(OH)_2$) was the primary oxidation product detected on the surface at potentials below 570 mV/SHE. At potentials exceeding 760 mV/SHE, elemental sulfur was also found to form on the mineral surface. Subsequently, Bruckard et al. [77] explored a potential-controlled flotation process as part of a three-stage treatment for arsenic-bearing copper minerals. This comprehensive treatment included

arsenic reduction, low-temperature roasting, and the immobilization of arsenic in ceramics. The study successfully demonstrated the economic feasibility of producing low-arsenic content concentrates.

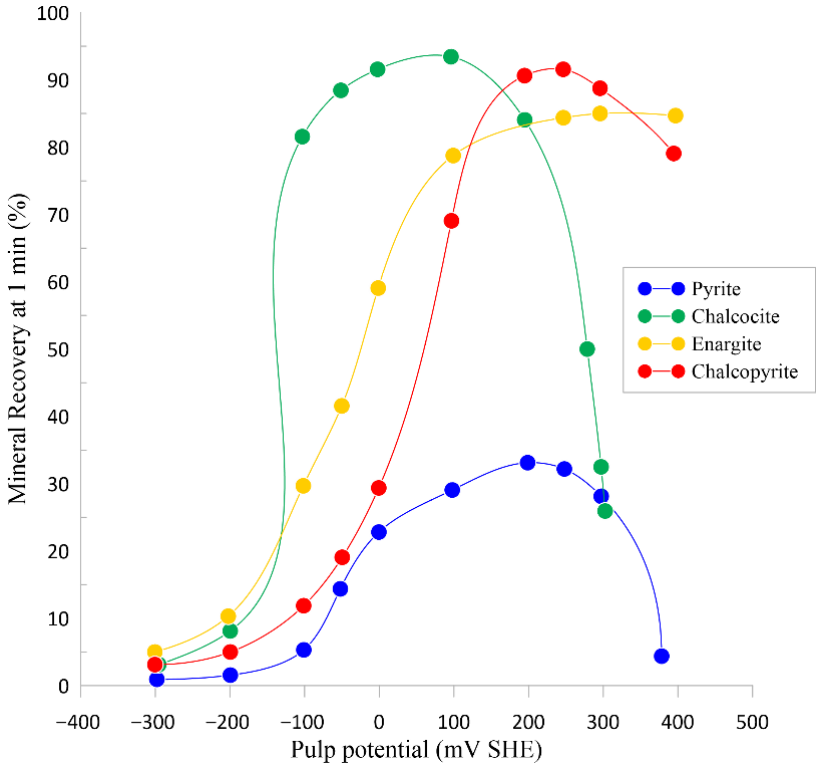

Figure 16. Mineral recovery at 1 min as a function of pulp potential for chalcopyrite, enargite, chalcocite, and pyrite at pH 11 (Adapted from [75]).

Comparatively, Smith et al. [78] presented case studies where pulp potential control was used to separate copper and arsenic minerals. They observed that tennantite floated from bornite and chalcopyrite within the pulp potential range between −200 and −130 mV/SHE. However, in other instances, limited recovery was noted for both arsenic-bearing minerals (tetrahedrite/tennantite) and non-arsenic copper minerals (chalcopyrite) under reducing potential conditions. Despite this, a separation window was identified at 400 mV/SHE, suggesting that effective separation might be achievable there. The efficiency of this separation and the selection of the optimal potential were highly dependent on the mineralogical characteristics of the ore samples [79]. Kappes and Gathje [80] further emphasized that detailed chemical and mineralogical analysis along with precise control over flotation chemistry are essential for an effective separation based on Eh and pH control.

Recent studies show promising advances in the selective flotation of enargite from complex ores using pulp potential control. For example, Tayebi-Khorami et al. [3,9] applied this technique to investigate the separation of enargite from other copper sulfides in the Tampakan copper-gold deposit in the Philippines. Their primary goal was to analyze enargite's floatability in ore samples with high and low arsenic content (HAS and LAS, respectively) under various potential conditions to assess the effectiveness of selective enargite separation. As Figure 17 illustrates, the most significant findings indicate a lower enargite recovery at Eh of −200 mV/SHE (47% for the HAS sample and 67% for the LAS sample). Recovery then gradually increased with rising Eh, reaching its maximum at 200 mV/SHE (62% for HAS and 82% for LAS). Subsequently, recovery decreased as Eh moved towards more oxidizing conditions (51% for HAS and 60% for LAS at 400 mV/SHE). The unexpectedly high recoveries at −200 mV/SHE for both enargite and non-enargite

copper (NECu) minerals are inconsistent with previous studies by Guo and Yen [8], and Senior et al. [75], which reported low or no enargite floatability below −100 mV/SHE. This discrepancy might be due to hysteresis effects related to pulp potential adjustment, a phenomenon supported by research from Smith and Bruckard [79] and consistent with the findings of Tayebi-Khorami et al. [3,9].

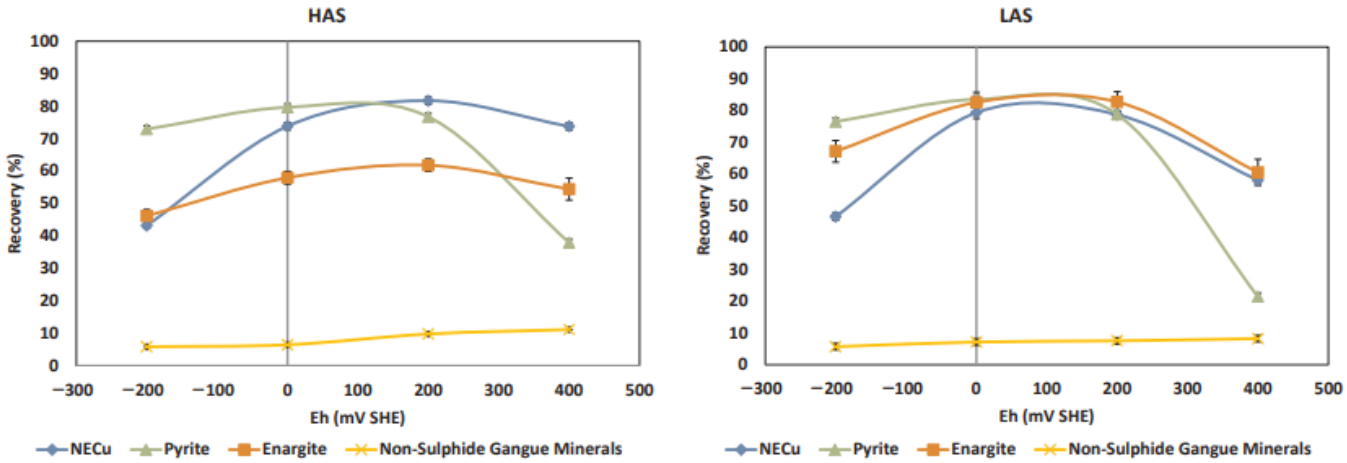

Figure 17. Unclassified mineral group recoveries after 10 min of flotation under different Eh conditions for HAS and LAS concentrates (ref. [9] with permission).

According to Senior et al. [75], enargite exhibits stronger floatability than chalcopyrite under slightly reducing conditions, suggesting the potential for selective separation (Figure 16). In the LAS sample, enargite showed a 67% recovery at −200 mV/SHE while NECu achieved 46%. This aligns with Smith et al. [78] findings for tennantite which can be separated from other non-tennantite copper minerals within this potential range. However, the same selectivity was not observed in the HAS sample as in this case enargite and NECu recoveries were similar between −200 and −130 mV/SHE, preventing effective separation. At 400 mV/SHE in the LAS sample, recoveries of both enargite and NECu decreased. This is consistent with observations by Smith and Bruckard [79] who noted that the floatability of tennantite and non-tennantite copper minerals declines above this potential. Under these oxidizing conditions, effective separation between enargite and NECu was not achieved. Conditioning at 400 mV/SHE created an excessive depressing effect, negatively impacting selectivity between the two minerals. In the HAS sample, enargite did not float as expected, showing minimal variation in recovery with increasing Eh. The difference between minimum and maximum recoveries was 15 percentage points, while in the LAS sample, it was 22 percentage points. Tayebi-Khorami et al. [3,9] theorize that the lower recovery in the HAS sample could be due to poor liberation, inadequate particle size, or hydrophilic surfaces caused by coatings or oxidation which is supported by Runge [81]. Additional tests were conducted to improve recovery in HAS by increasing flotation time and collector dosage, achieving maximum recovery of 68%, in contrast to 93% in the LAS sample under the same conditions.

In a subsequent study, Tayebi-Khorami et al. [82] conducted surface chemistry analyses using EDTA extraction on HAS and LAS samples. Their goal was to clarify the recovery differences previously reported by Tayebi-Khorami et al. [3,9]. The authors demonstrated that strong galvanic interactions between enargite and pyrite in the HAS sample led to enargite's oxidation. This oxidation reduced its floatability and negatively affected its selectivity compared to other copper minerals. This finding aligns with previous research highlighting the significant impact of galvanic interactions between sulfide minerals [83–88].

Previous research suggested that galvanic interactions promote the formation of iron hydroxide species on mineral surfaces [89] and that both galvanic interactions and redox reactions in the pulp are primary drivers for the precipitation of iron oxyhydroxide species on sulfide mineral surfaces, ultimately leading to reduced sulfide mineral floatability [90]. Tayebi-Khorami et al. [82] confirmed these phenomena in the selective flotation of enargite from other sulfides which is consistent with earlier studies [23,33,40,91–94].

Their work showed that enargite has the lowest rest potential compared to other sulfide minerals in the HAS and LAS ore samples, following the following order: pyrite > chalcopyrite > bornite > enargite. According to this rest potential order, the strongest galvanic interaction occurs between enargite and pyrite, causing significant enargite oxidation which creates a hydrophilic oxidation layer that depresses flotation [87,95–97]. Additionally, a substantial amount of copper ions are dissolved, enough to activate pyrite at pulp potentials below 400 mV/SHE, thus contributing to the low recovery of enargite in the HAS sample. As the pulp potential increased above 400 mV/SHE, enargite experienced even stronger galvanic interactions with pyrite which resulted in decreased pyrite floatability due to the precipitation of hydrophilic iron hydroxides on its surface, further contributing to its depression in the flotation process.

Table 2 shows a summary of the different studies on the use of pulp potential and pH control in the selective flotation of enargite from other sulfides.

Table 2. Summary of various studies on pulp potential control for selective flotation of enargite.

Source	Research Objectives	Main Results
[68]	Evaluate the floatability of enargite as a function of pulp potential using hydrogen peroxide and sodium sulfide.	Enargite floats without a collector under oxidizing conditions and it is depressed under reducing conditions. Maximum recovery occurs between 150 and 270 mV/SHE.
[8]	Analyze the floatability of enargite and chalcopyrite in simple and mixed- mineral systems under different potentials.	Enargite floatability remains stable between −100 and 450 mV/SHE, decreasing outside this range.
[74]	Evaluate the flotation range of enargite using different collectors, comparing PAX and NaEtX.	It expands the flotation range of enargite with PAX compared to NaEtX.
[75]	Investigate the separation of enargite from other copper minerals through pulp potential control.	The threshold flotation potential of enargite is −75 mV/SHE at pH 8.0 and −25 mV/SHE at pH 11.0. Its selective separation from chalcopyrite occurs at 0 mV/SHE (pH 8.0 or 11.0).
[76]	Analysis of the effect of pH and pulp potential on the flotation of metallic arsenic using ethyl xanthate.	Arsenic exhibited high floatability (up to 95% recovery in 8 min) with Aerofroth 65 and 40 g/t of PEX at pH 5.0–10.0. At pH 10.0, its flotation was efficient within a potential range of −300 to 225 mV/SHE.
[43]	Identify the formation of passivating layers in the flotation of arsenic at different potentials.	Identification of a $Cu(OH)_2$ passivating layer at potentials <570 mV/SHE and elemental sulfur at potentials >760 mV/SHE.
[3,9]	Evaluate the floatability of enargite in high- and low-arsenic content samples under different pulp potentials.	Enargite exhibits a lower recovery at −200 mV/SHE and maximum recovery at 200 mV/SHE.
[82]	Analyze the galvanic interactions between enargite and pyrite and their impact on selective flotation.	Galvanic interactions with pyrite oxidize enargite, reducing its floatability and affecting selectivity.

3.3. Reagents for Selective Oxidation of Enargite

Mineral surface oxidation is a fundamental process in sulfide flotation that directly impacts floatability. Mild oxidation of the mineral surface can facilitate collector adsorption and the formation of elemental sulfur, which increases the mineral's hydrophobicity [98]. However, more intense oxidation generates products like oxides and metal hydroxides which act as physical barriers, hindering collector adsorption and ultimately reducing floatability [99,100]. Therefore, maintaining appropriate control between mild and excessive oxidation is essential for optimizing the selectivity and efficiency of the enargite flotation process.

Huch [101] developed and patented a froth flotation method for the separation of chalcocite and enargite, a technique also applicable to other copper minerals. This innovative method involves treating a mineral suspension with an oxidizing agent, preferably H_2O_2, followed by precise pH adjustment. The primary objective is to enhance the floatability of enargite while simultaneously depressing chalcocite. The process begins with the controlled addition of the oxidant, maintaining the Eh (redox potential) between 50 and 200 mV/SHE to ensure optimal separation. The suspension then progresses through multiple monitored tanks, where the Eh levels are gradually fine-tuned with additional oxidant. Subsequently, the pH is adjusted using either lime or an acid, such as sulfuric acid, a choice dependent on the type of collector to be employed in the subsequent flotation stage. A frother, like MIBC, and a copper collector, such as xanthate, are then introduced. This carefully managed sequence facilitates the flotation of enargite, allowing it to be recovered, while chalcocite settles to the bottom of the tank. To achieve higher purity, both resulting concentrates may undergo a second flotation stage. This process significantly leverages the inherent differences in mineral oxidizability, thereby enabling a more efficient separation compared to traditional flotation methods.

Fornasiero et al. [7] conducted a study on the flotation separation of chalcocite, covellite, and chalcopyrite from enargite or tennantite in mixed mineral systems, focusing on the selective oxidation of mineral surfaces and the dissolution of their oxidation products. They conditioned minerals under both non-oxidizing conditions with N_2 gas (at pH 5.0 and 11.0) and oxidizing conditions with O_2 gas and H_2O_2 (at pH 5.0 and 11.0), adding the collector after conditioning with EDTA at pH 11.0 to selectively remove surface oxidation products. While non-oxidizing conditions with N_2 at pH 5.0 yielded high recovery for all minerals without selectivity, pH 11.0 showed relatively good separation between chalcopyrite and tennantite, chalcopyrite and enargite, and between covellite and tennantite. Conversely, separating chalcocite from enargite and tennantite was less effective, indicating that the presence of a full range of copper minerals in a real flotation system may lead to poor separation between copper and arsenic minerals. Under oxidizing conditions, better separation of arsenic-bearing and non-arsenic minerals was achieved through selective oxidation with H_2O_2 at both pH 5.0 and pH 11.0, followed by the addition of EDTA to remove surface oxidation products, as shown in Figures 18 and 19. At pH 5.0, arsenic-bearing minerals oxidize more readily than non-arsenic minerals, and arsenic oxides are more stable than copper oxides. However, at pH 11.0, EDTA preferentially dissolves copper oxide, favoring the flotation of non-arsenic minerals. Figure 18 shows that, after conditioning with H_2O_2 at pH 5.0, higher flotation recovery was achieved in non-arsenic minerals (47%–82%) compared to arsenic-bearing minerals (40%–53%), allowing for good separation, particularly in systems containing enargite. XPS analysis results reveal that the proportion of copper oxide on the surface is lower at pH 5.0 than at pH 11.0, explaining the higher recoveries at pH 5.0. The higher proportion of arsenic oxides on the surface at pH 5.0 and their reduced dissolution also contribute to this improved separation, consistent with observations by Marasinghe and Koleini [102].

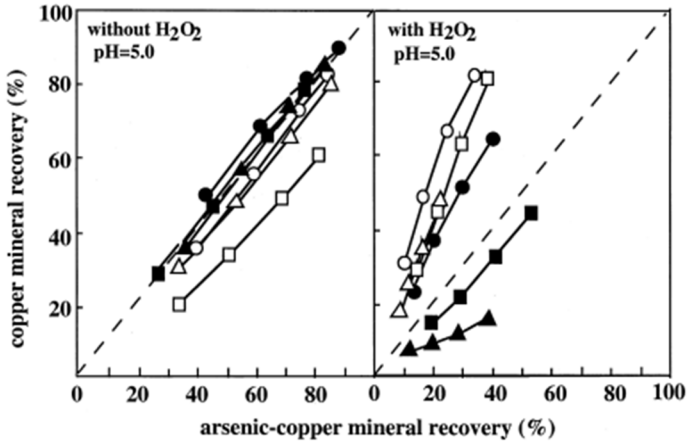

Figure 18. Flotation recoveries of mixed mineral systems represented by open circles (chalcocite-enargite), open squares (covellite-enargite), open triangles (chalcopyrite-enargite), filled circles (chalcocite-tennantite), filled squares (covellite-tennantite), and filled triangles (chalcopyrite-tennantite) at 1, 2, 4, and 8 min at pH 5, without (N_2 conditioning 20 min) and with 0.013 wt% H_2O_2 (60 min O_2 conditioning); mineral concentration: 5 g/dm^3; DEDTP = 2 × 10^{-5} mol/dm^3 (ref. [7] with permission).

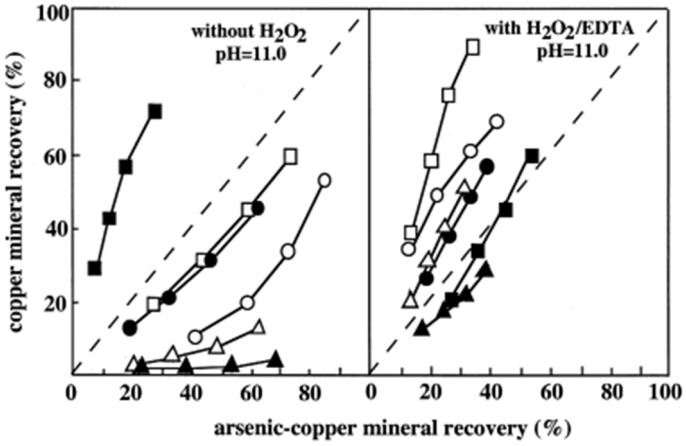

Figure 19. Flotation recoveries of mixed mineral systems represented by open circles (chalcocite-enargite), open squares (covellite-enargite), open triangles (chalcopyrite-enargite), filled circles (chalcocite-tennantite), filled squares (covellite-tennantite), and filled triangles (chalcopyrite-tennantite) at 1, 2, 4, and 8 min at pH 11, without (N_2 conditioning 20 min) and with 0.013 wt% H_2O_2 (60 min O_2 conditioning); EDTA = 4.5 × 10^{-4} mol/dm^3; mineral concentration: 5 g/dm^3; DEDTP = 2 × 10^{-5} mol/dm^3 (ref. [7] with permission).

Li et al. [103] investigated the separation of enargite from NECu minerals analyzing the effects of regrinding, pH, NaClO concentration, conditioning time, and flotation time on. Their flotation results shown in Figure 20A indicated that NaClO affected the recovery of enargite and NECu minerals. Without NaClO, recoveries were 57.8 and 60.7%, respectively, with low separation selectivity (0.95). At NaClO concentrations of 0.5% (v/v), NECu recovery drastically decreased, and further increased in NaClO concentration had a negligible effect on NECu recovery. On the other hand, arsenic recovery gradually increased at NaClO concentrations below 0.5%, then decreased at higher concentrations, indicating that enargite was also depressed under strong oxidation conditions. This behavior is attributed to the formation of hydrophilic species investigated by Plackowski et al. [37,39]. Regarding conditioning time, as shown in Figure 20B, NECu recovery gradually decreased as conditioning time increased, while arsenic recovery showed a slight increase between 5 and 10 min. However, extending the conditioning time to 30 min reduced arsenic recovery to 49%.

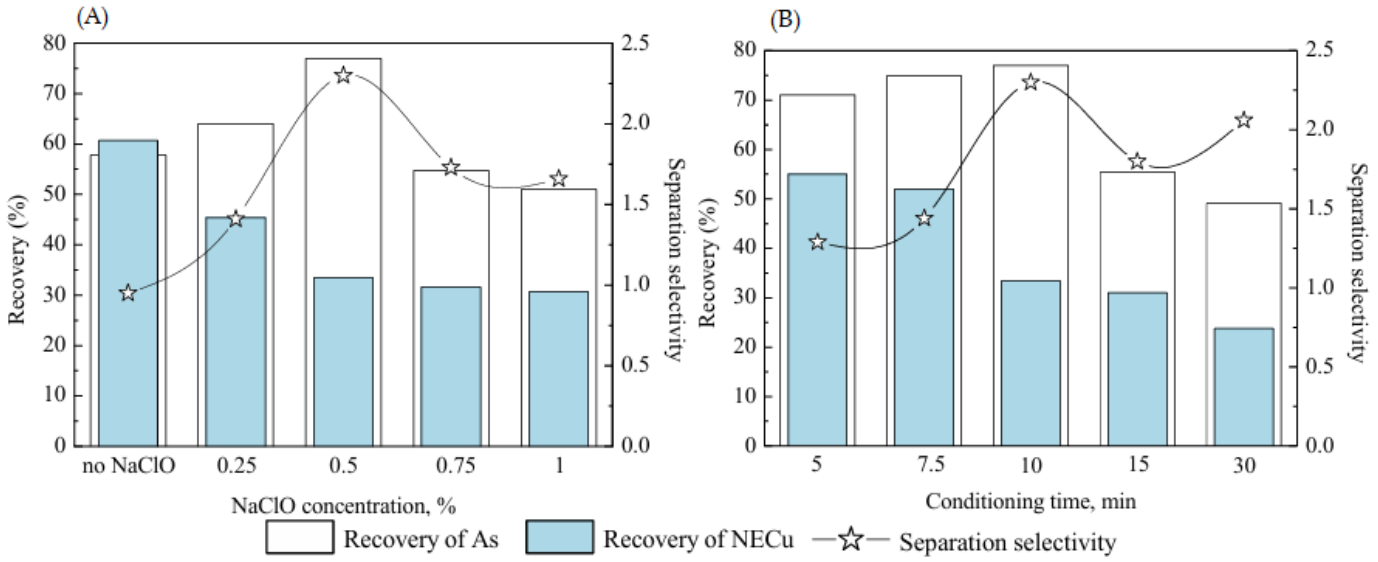

Figure 20. Effect of (**A**) NaClO concentration and (**B**) conditioning time on the separation of enargite from NECu minerals with NaClO concentration varied in the range of 0 to 1.5% (ref. [103] with permission).

Li et al. [103] also studied the effect of EDTA (Figure 21) treatment and showed that at pH 11.6 it improved the floatability of both minerals by dissolving surface oxidation products, a finding consistent with that reported by Fornasiero et al. [7]. Li et al. [103] suggested that NECu minerals were more oxidized than enargite during the conditioning stage. However, selectivity between enargite and NECu decreased after EDTA treatment, demonstrating the selective oxidation of NECu minerals under oxidizing conditions. These authors proposed a conceptual flow diagram for separating enargite from the complex minerals, as illustrated in Figure 22. The process involves further grinding of the concentrate, pH adjustment, and NaClO treatment to separate high- and low-arsenic copper, followed by flotation and hydrometallurgical processing. The final low-arsenic concentrate is then sent for smelting.

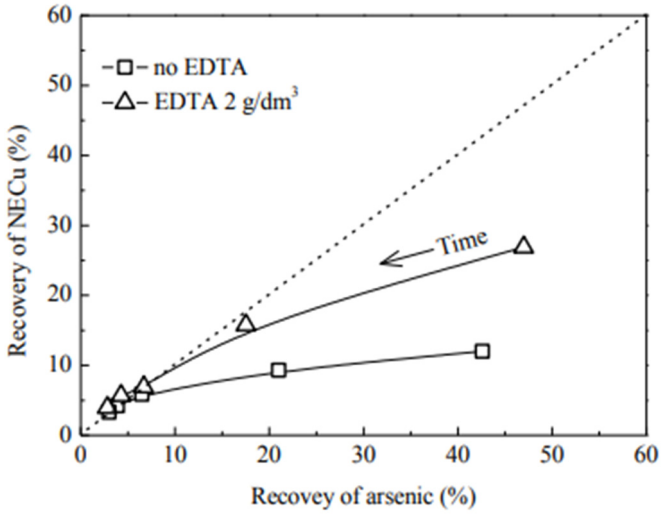

Figure 21. Flotation recovery of arsenic and NECu as a function of flotation time. Flotation conditions: regrinding 5 min, pH 11.6, 0.5% (*v*/*v*) NaClO, and conditioning time 10 min (ref. [103] with permission).

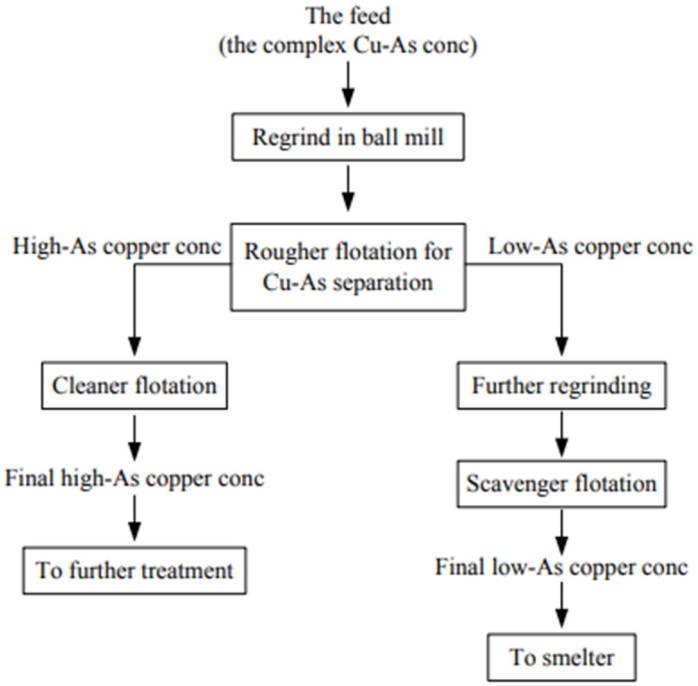

Figure 22. Proposed conceptual flow diagram for the separation of enargite from non-arsenic copper minerals (NECu) (ref. [103] with permission).

Suyantara et al. [65] investigated the effect of H_2O_2 oxidation treatment on the floatability of copper sulfide minerals (chalcopyrite and bornite) and arsenic-bearing copper minerals (tennantite and enargite), in the presence and absence of PAX. Results for the pure mineral system showed that, without oxidation, all minerals exhibited moderate natural floatability, similar to that reported by Kantar [68], Petrus et al. [104], and Smith and Heyes [78] under alkaline conditions. Following the treatment with 0.1 mM H_2O_2 showed that the floatability of chalcopyrite and bornite slightly increased, while that of enargite and tennantite decreased, suggesting a faster oxidation rate in the latter minerals. At higher H_2O_2 concentrations (above 1.0 mM), the floatability of all minerals decreased, with complete depression observed, attributed to the formation of hydrophilic species on the surface due to surface oxidation. Adding 0.1 mM PAX improved the recovery of all minerals, even after oxidation with H_2O_2 at low concentrations (0.1 and 1 mM). However, at higher H_2O_2 concentrations (10 mM), recovery decreased significantly, particularly in tennantite, whose recovery dropped from 70 to less than 20%. Recovery remained low after treating minerals with 100 mM H_2O_2 and PAX, likely due to intense surface oxidation and PAX degradation under highly oxidizing conditions.

For the mixed mineral system, results showed that, overall, the recovery of these minerals decreased as the H_2O_2 concentration increased, although a slight increase was observed at specific concentrations. In chalcopyrite-enargite (Cp-En) and chalcopyrite-tennantite (Cp-Tn) mixtures, the floatability of chalcopyrite was significantly depressed with the addition of 0.1 mM PAX in the presence of different H_2O_2 concentrations. At the same time, enargite and tennantite exhibited higher floatability, suggesting the possibility of selective flotation. Newton efficiencies for the Cp-En and Cp-Tn mixtures indicate that the optimal H_2O_2 concentrations to separate chalcopyrite-enargite and chalcopyrite-tennantite are 0.1 mM and 0.2 mM in the presence of 0.1 mM PAX, respectively. In bornite-enargite (Bn-En) and bornite-tennantite (Bn-Tn) mixtures, floatability was also observed, reaching a maximum at H_2O_2 concentrations of 1 mM, after which it declined.

In the Bn-Tn mixtures, bornite recovery increased significantly at higher H_2O_2 concentrations, possibly due to the formation of oxidized copper products that enhanced PAX

adsorption. Newton efficiencies for the Bn-En and Bn-Tn mixtures indicate that the optimal H_2O_2 concentrations for separating bornite-enargite and bornite-tennantite in the presence of 0.1 mM PAX are 0.5 mM and 0.2 mM H_2O_2, respectively.

Gan et al. [52] investigated the effect of oxidation treatment using a mixture of NaClO and $FeCl_3$ on the flotation separation of covellite and enargite. Microflotation tests, contact angle measurements, laboratory-scale flotation, XPS and SEM analyses were conducted to characterize the separation of both minerals. The results demonstrated successful separation at pH levels above 10.0, with the sequential addition of NaClO and $FeCl_3$ enhancing the hydrophobicity difference between covellite and enargite, as indicated by microflotation and contact angle measurements. The optimal dosage ratio of NaClO to $FeCl_3$ was found to be 4:1, with conditioning times of 30 min for NaClO and 10 min for $FeCl_3$, yielding the best separation results. In the laboratory-scale flotation tests, the bulk copper concentrate was divided into two fractions: one with low arsenic content (0.46%) and another with high arsenic content (5.18%). XPS and SEM analyses revealed that NaClO treatment promoted oxide accumulation on the surface of covellite, whereas this effect was not observed on enargite. Additionally, since $FeCl_3$ acts as an oxidant and a flocculant, hydrophilic ferric hydroxide colloids formed in the solution. The selective adsorption of ferric hydroxide on the surfaces of covellite and enargite further intensified the difference in floatability between the two minerals, facilitating their separation. The authors argue that the described oxidation treatment is feasible for reducing arsenic content in copper concentrates. However, they note that further research is required to lower the reagents' costs.

García-Garnica et al. [48] conducted an electrochemical characterization of enargite oxidation within a potential window correlated with the mixed potential achieved using oxidizing reagents such as hydrogen peroxide (H_2O_2), NaClO, calcium hypochlorite ($Ca(ClO)_2$), and $KMnO_4$, comparing these results with those for chalcopyrite under similar conditions. The results showed that, although enargite is more challenging to oxidize in alkaline media (pH 10.0 and 11.0), it achieved more positive mixed potentials than chalcopyrite under the same experimental conditions. Additionally, the differences in the recorded potentials with the various oxidants underscore the importance of the mixed potential concept, as the reagents generate different effects in solution and on the mineral surface. At pH $\geq$ 10.0, the reactivity order for enargite is $Ca(ClO)_2 > KMnO_4 > NaClO > H_2O_2$. A voltammetric study was conducted by García-Garnica et al. [48] using a natural enargite electrode under two conditions: (i) without prior conditioning (AO), and (ii) after three minutes of surface conditioning with different oxidizing reagents. It was found that hypochlorite reagents were the most effective in generating a more significant potential difference between the two minerals. The most considerable potential differences were observed at pH 10.0. The results showed that NaClO was the most suitable oxidizing reagent for potential control in the flotation process. Another significant result is that enargite oxidation achieved with any oxidizing reagents would produce $Cu(OH)_2$, thereby rendering the surface hydrophilic. In contrast, for chalcopyrite, the oxidizing reagents cannot reach the potential required to oxidize the surface to $Cu(OH)_2$, as shown by the cathodic responses, and thus oxidation results in copper polysulfides that increase its hydrophobicity. Accordingly, generating a hydrophilic surface on enargite within the potential window of 200 to 500 mV/SHE ensures its depression while producing a hydrophobic surface on chalcopyrite.

In a recent study on the selective flotation of copper concentrates containing arsenic, Suyantara et al. [105] investigated the effects of PAX and oxidation treatment using H_2O_2 on the selective flotation of copper concentrates containing arsenic-bearing copper minerals under various pH conditions (Figure 23). X-ray diffraction (XRD) analysis determined that

the copper–arsenic concentrate was mainly composed of chalcopyrite as the primary copper sulfide mineral, enargite as the main arsenic-bearing copper mineral, and pyrite, and quartz as gangue minerals. Additionally, 60% of the copper–arsenic concentrate consisted of fine particles smaller than 38 µm, concentrating approximately 63% of the arsenic and 64% of the copper. The results demonstrated that the addition of 60 g/t of PAX and oxidation treatment with 0.1 M H_2O_2 improved the selective separation of copper sulfides and arsenic-bearing copper minerals by enhancing the flotation recovery of arsenic-bearing copper minerals. Based on these results, Suyantara et al. [105] proposed a new flotation process to separate copper minerals and arsenic-bearing copper minerals, generating a "dirty" copper concentrate with high arsenic content and a "clean" copper concentrate with low arsenic content in the tailings, as illustrated in Figure 24. The "dirty" concentrate can be further processed to extract copper from arsenic-bearing minerals, while the "clean" concentrate is suitable for smelting.

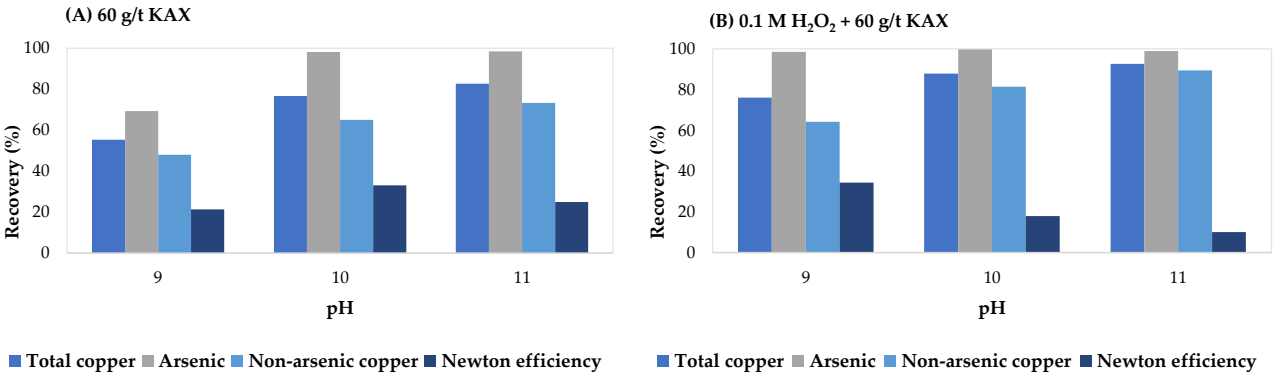

Figure 23. Effect of pH on total copper, arsenic, arsenic-free copper recoveries, and Newton efficiency after 30 min of flotation. Copper concentrates containing arsenic-bearing copper minerals were treated with (**A**) 60 g/t of KAX and (**B**) a combination of an aqueous H_2O_2 solution at 0.1 M and 60 g/t of KAX under various pH conditions (Adapted from [105]).

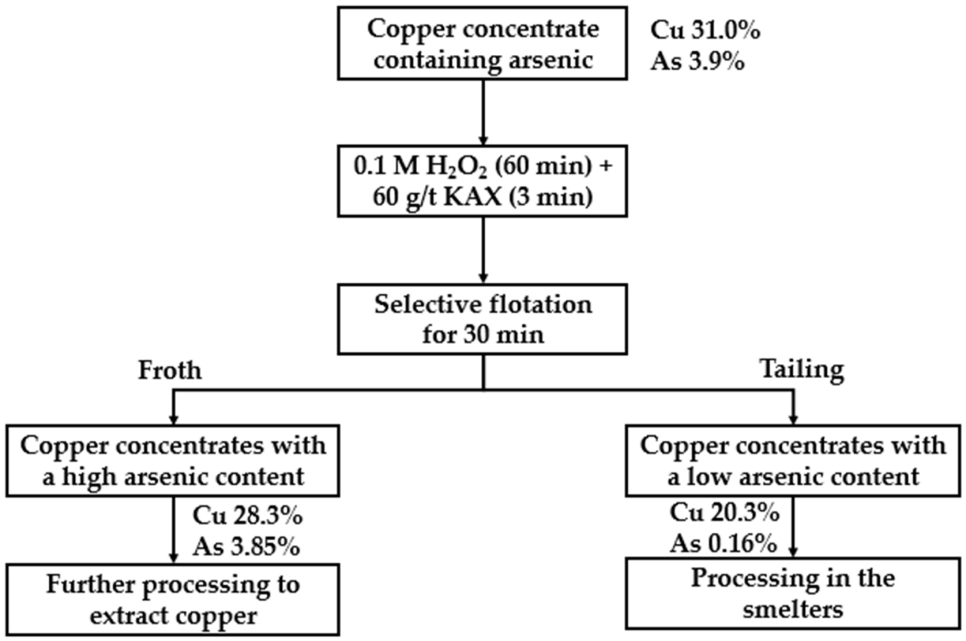

Figure 24. Proposed selective flotation process scheme for the separation of arsenic-bearing copper minerals from copper concentrates, using H_2O_2 oxidation treatment and the addition of KAX at pH 9 (Adapted from [105]).

Regarding the mechanism of action of the oxidizing agent, Suyantara et al. [106] proposed that the selective flotation of enargite and chalcocite in the presence of low concentrations of H_2O_2 and PAX is governed mainly by differences in the adsorption of the reactant and the surface oxidation products. PAX adsorbs more rapidly on enargite than on chalcocite, forming CuAX and $(AX)_2$ species on the enargite surface. In contrast, chalcocite exhibits slower adsorption and a lower proportion of these collector species. Oxidation with H_2O_2 promotes the formation of Cu(II) hydroxides and sulfate species in both minerals, along with arsenic oxides (As_2O_3 and As_2O_5) in enargite. The relative proportions and spatial distribution of xanthate complexes, polysulfides, and oxidized species on the mineral surfaces explain the observed flotation selectivity, as schematically illustrated in Figure 25.

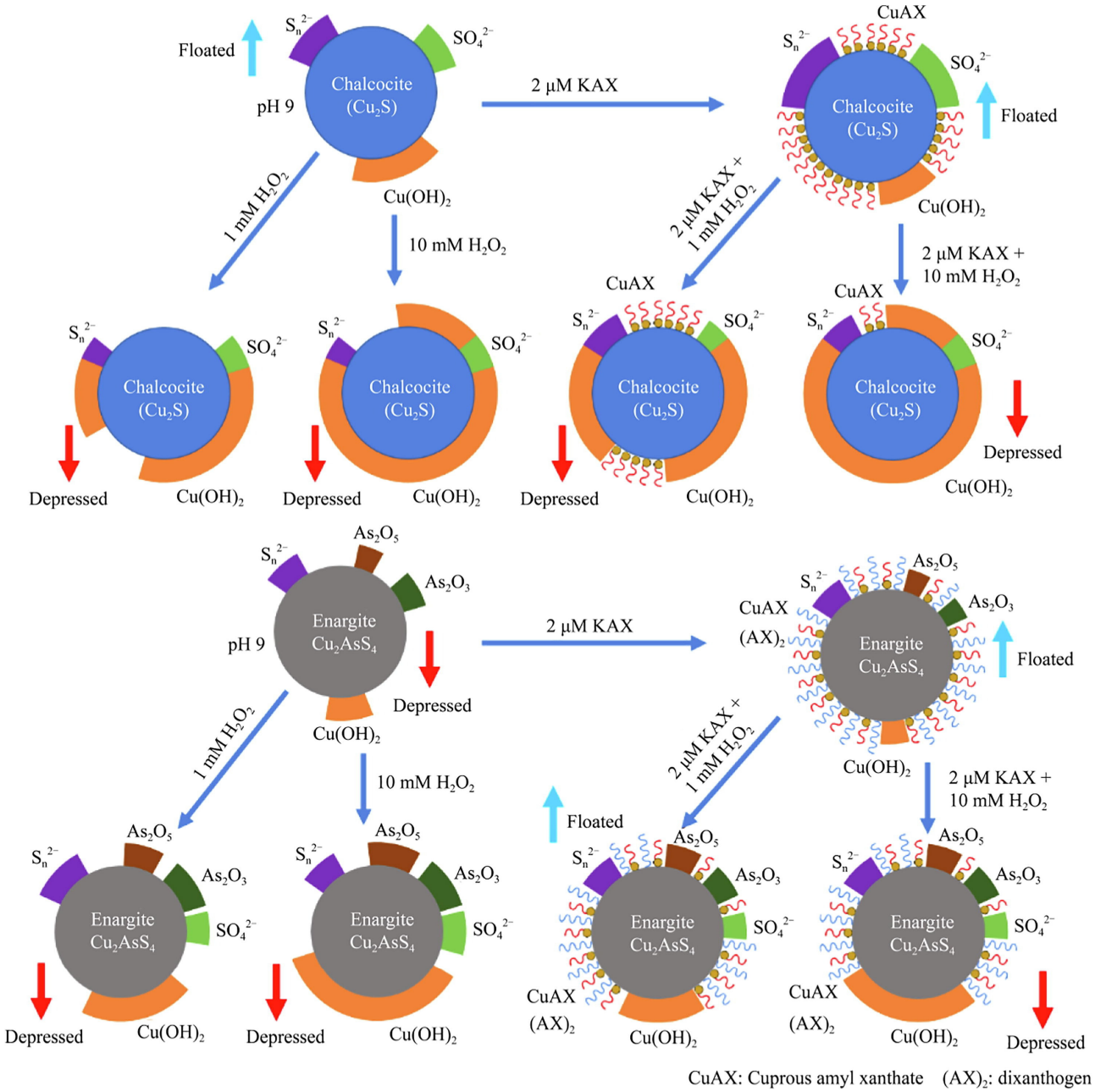

Figure 25. A proposed surface mechanism for chalcocite and enargite before and after the H_2O_2 treatment in 0 and 2 lM KAX at pH 9 (ref. [106] with permission).

3.4. Flotation of Enargite in Seawater

A significant challenge in mining is the scarcity of water for copper mineral processing, which has led to the use of seawater as a viable alternative. The flotation behavior of copper sulfides and molybdenite in seawater has been investigated, showing that molybdenite flotation is negatively affected at pH > 9.5 when lime is used to depress pyrite, due to the formation of Mg^{2+} hydrolysis products, while copper sulfides remain unaffected [107,108]. Dispersants have shown positive results in removing magnesium hydroxides from the molybdenite surface [109]. However, only a few publications address the flotation behavior of enargite in seawater which highlights a significant research gap.

Yepsen et al. [110] studied the behavior of enargite in the flotation process using seawater and compared the flotation of enargite and chalcopyrite in this aqueous medium. Enargite recovery as a pH function was evaluated in a 0.01 M NaCl solution (low ionic strength water) and seawater. In the NaCl solution, enargite recovery remained constant throughout the studied pH range, with a reduction in electrochemical potential (Eh) and dissolved oxygen as pH increased. In contrast, in seawater, enargite flotation was lower compared to low ionic strength water, and although recovery remained stable between pH 8.0 and 10.0, a marked depression was observed at pH values above 10, also accompanied by a decrease in Eh and dissolved oxygen (Figure 26). This behavior was attributed to the strong depressing effect of magnesium on enargite, especially at pH > 10.0, while calcium ions also reduce recovery at that pH, though to a lesser extent. Both effects are attributed to the hydrolysis products of these divalent cations. These findings were further supported by Pourbaix diagrams analyses for the As-Ca and As-Mg systems shown in Figure 27 and the distribution of arsenate species in seawater shown in Figure 28, which indicate that at pH > 9.0 and Eh between −120 and −130 mV/SHE, hydrophilic species such as $Ca(AsO_2)_2$, $Ca_3(AsO_4)_2$, $Mg(AsO_2)_2$, and $Mg_3(AsO_4)_2$ are likely to form on the enargite surface. This suggests that the depression of enargite at pH > 9.0 is due not only to the adsorption of magnesium and calcium hydroxyl complexes but also to the interaction of these cations with oxidized arsenic species, such as arsenate and arsenite.

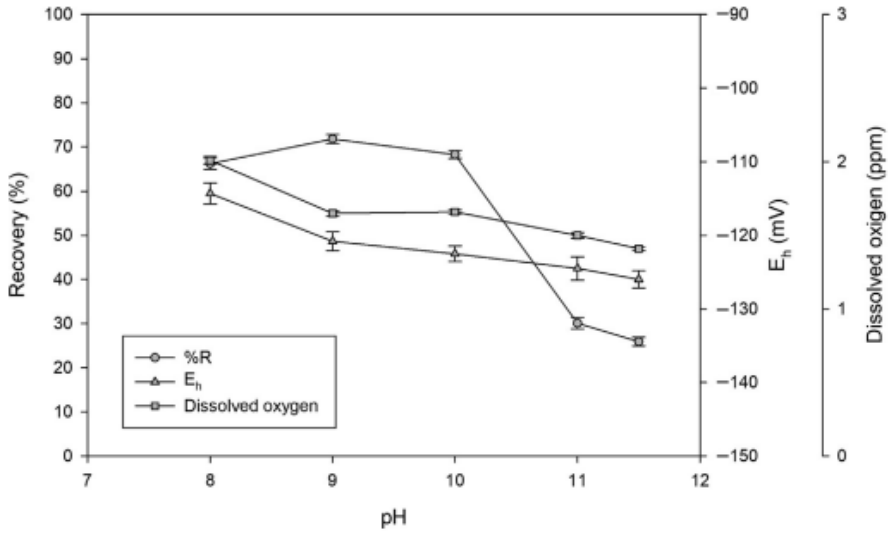

Figure 26. Enargite recovery as a function of pH in seawater using 25 ppm of PAX and 30 ppm of MIBC (ref. [110] with permission).

The authors also compared the flotation of enargite and chalcopyrite using seawater. The results show that chalcopyrite flotation is unaffected in a 0.01 M NaCl solution, remaining constant across the studied pH range, although Eh and dissolved oxygen decrease as pH increases. In seawater, chalcopyrite flotation is slightly lower than observed in NaCl

and, as with enargite, remains stable below pH 10.0 but experiences an intense depression under more alkaline conditions, accompanied by a reduction in Eh and dissolved oxygen.

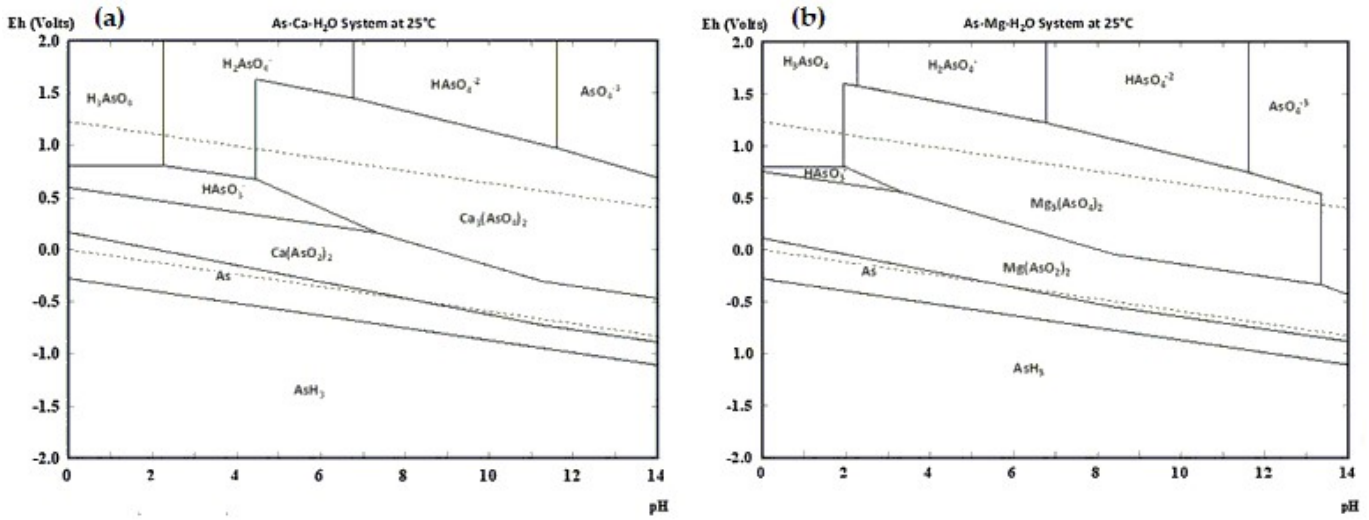

Figure 27. Pourbaix diagram for (**a**) the Ca-As system and (**b**) the Mg-As system. Data obtained from HSC V6.00 software (ref. [110] with permission).

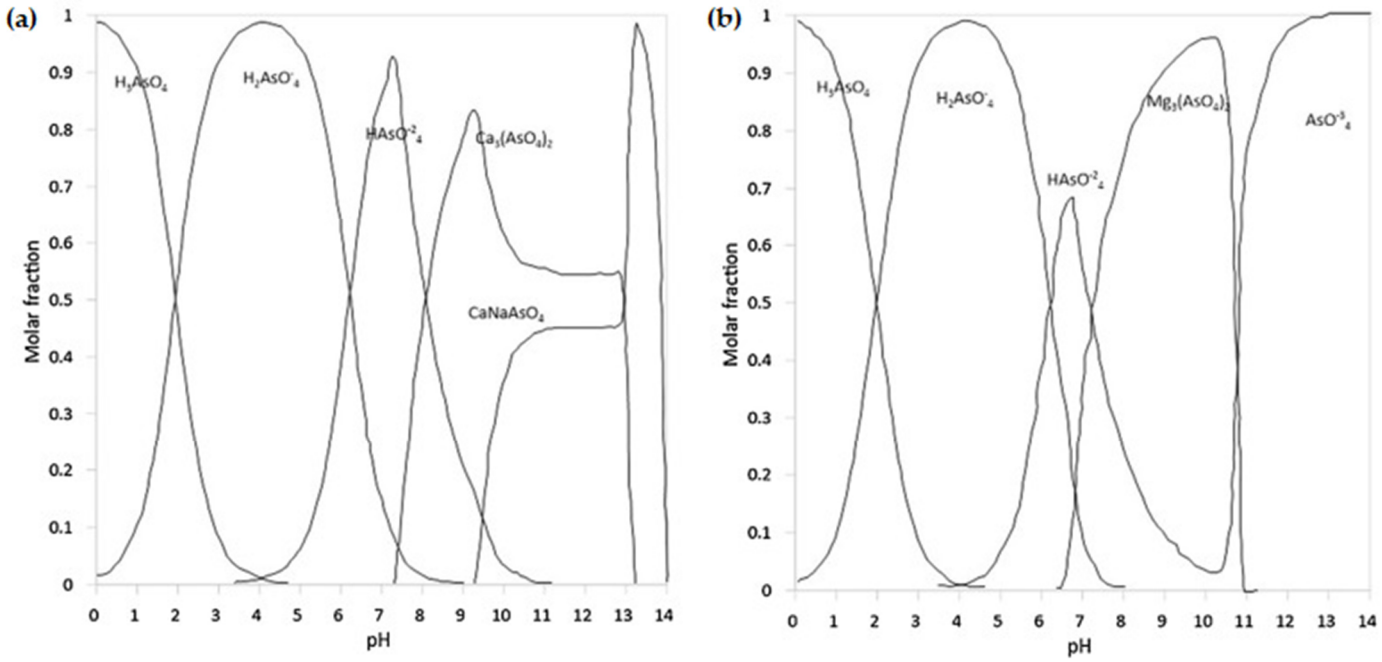

Figure 28. Distribution of arsenate species in seawater conditions for (**a**) Ca^{2+} and (**b**) Mg^{2+} (Adapted from [111] with permission).

In a subsequent study, Yepsen and Gutierrez [10] expanded the study conditions, describing the flotation behavior of enargite in seawater under different pulp electrochemical potentials (Eh) and pH levels. The independent effects of calcium and magnesium were also evaluated. The results shown in Figure 29 indicate that enargite recovery in seawater at pH 9.0 is approximately 15 percentage points lower than that obtained with a pH 10.0 buffer solution, with an intense depression under oxidizing conditions (Eh > 100 mV). In the reducing range, recovery in seawater is also lower than in the buffered solution. At pH 10.5 in seawater, a significant depression is observed across the entire Eh range, attributed to the adhesion of magnesium hydrolysis products on the enargite

surface, rendering it hydrophilic [110,112]. However, previous studies also showed that thiol-type collectors such as PAX can degrade due to dissolved calcium in seawater [113]. Thus, the results obtained in the presence of seawater contrast with those obtained in the buffer solution at pH 10.0.

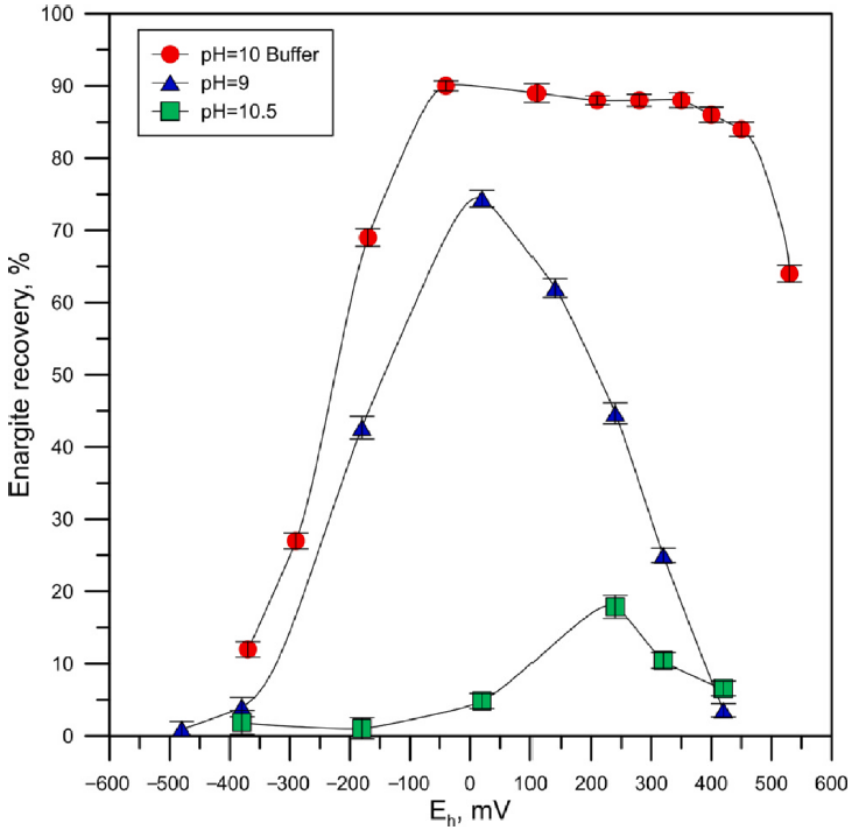

Figure 29. Enargite recovery as a function of Eh in seawater, at pH 9 and 10.5. Results obtained using the buffer solution at pH 10 are also included (ref. [10] with permission).

The depressing effect of calcium on enargite flotation is stronger than the depressing effect of magnesium, even though calcium concentration in seawater is lower. This strong effect of these cations can be explained by the presence of hydrophilic arsenates ($Ca_3(AsO_4)_2$, $Mg_3(AsO_4)_2$, $Ca_3(AsO_4)_2{\cdot}H_2O$, $Mg_3(AsO_4)_4{\cdot}H_2O$) on the enargite surface, which may form under oxidizing conditions. SEM-EDS analyses indicate the presence of calcium-rich precipitates at all tested Eh levels, explained by the high stability of calcium arsenates compared to magnesium arsenates. Another significant result is the difference in flotation recoveries between chalcopyrite and enargite under oxidizing conditions, where chalcopyrite shows a more pronounced decrease across all experimental conditions. Yepsen and Gutierrez [10] theorize that this behavior could be due to differences in the electrical resistivity properties of both minerals, as suggested by Guo and Yen [8].

4. Research Opportunities

To advance the understanding and optimization of the selective flotation of enargite from other copper sulfide minerals, it is essential to identify and address critical research gaps that currently limit the efficiency and reliability of existing separation methods. These gaps represent key areas where further investigation could lead to the development of more selective and environmentally sustainable flotation strategies. The most relevant of these research needs, which hold potential for significantly improving mineral separation performance, are outlined in the following sections.

4.1. Electrochemical Effect of Pyrite

The galvanic interaction between enargite and pyrite remains a relatively unexplored area that could benefit from targeted electrochemical studies under plant-relevant conditions. Future research should quantify how galvanic coupling between copper and arsenic sulfides affects selective flotation kinetics, redox potential (Eh) stability, and mineral oxidation rates in complex ore matrices. Evaluating these effects under real operating conditions in flotation plants with complex mineral systems, where multiple sulfide species interact simultaneously, would be essential. Applying electrochemical impedance spectroscopy (EIS) and open-circuit potential monitoring in mixed-mineral pulp systems could bridge the gap between pure mineral experiments and plant-scale scenarios. Such studies would clarify the extent to which galvanic effects contribute to the inconsistencies observed in reported optimal separation conditions for arsenic-bearing versus non-arsenic-bearing minerals.

4.2. Surface Modification by Oxidation

Detailed surface characterization of enargite conditioned with different oxidizing agents, under controlled pulp Eh, remains a priority. Techniques such as SEM–EDS, QEMSCAN, and AFM coupled with Raman spectroscopy can be applied to monitor changes in morphology, elemental composition, and surface topography. At the same time, XPS can identify specific reaction products and assess collector adsorption patterns. Testing oxidants across defined Eh–pH domains and correlating surface phase assemblages with flotation outcomes will enable optimized process control and improved selectivity in mineralogically complex feeds.

4.3. Optimization of Selective Reagents

Despite advances in using reagents such as PAX and oxidizing agents (H_2O_2, NaClO), it is essential to continue investigating new reagents or combinations that enhance selectivity in separating enargite and other copper sulfides. In particular, exploring the effect of alternative depressants that provide better control over the oxidation products formed on the enargite surface would be beneficial. Additionally, using EDTA has proven effective in dissolving surface oxidation products [7,82,103]. Further studies could explore its combination with different collectors and oxidants, as well as the evaluation of other chemical chelators to improve the separation between arsenic-bearing and non-arsenic copper minerals.

4.4. Ultrafine Particles

The behavior of fine (<38 μm) and ultrafine enargite and chalcopyrite particles under different milling, oxidation, and reagent regimes requires in-depth investigation. Future studies should integrate advanced particle characterization (e.g., laser diffraction, automated SEM liberation analysis) with flotation tests under high-energy and column flotation configurations. Researchers should focus on improving bubble–particle collision and attachment probabilities for ultrafines, potentially through nanobubble technology, hydrodynamic optimization, or selective flocculation strategies [114,115]. Enhancing the recovery of these particle fractions could substantially reduce arsenic levels in final copper concentrates while improving overall metallurgical performance.

4.5. Seawater

Results regarding the flotation of enargite in seawater indicated that enargite recovery decreases considerably under oxidizing and alkaline conditions due to the formation of hydrophilic calcium and magnesium compounds on its surface [10,110]. To improve its

floatability in seawater, it would be relevant to investigate the use of dispersants or surface modifiers that inhibit the adsorption of these complexes. In particular, reagents such as sodium hexametaphosphate or polyphosphate, which have shown effectiveness in other flotation systems, could be evaluated to reduce the adsorption of calcium and magnesium ions on the enargite surface.

4.6. Collector Stability in Saline Environments

Given that the degradation of thiol collectors such as PAX in the presence of calcium and magnesium ions has been documented, it is relevant to investigate mechanisms to mitigate this effect. Exploring both the use of modifiers and pretreatment strategies capable of protecting collectors from decomposition in seawater environments would be valuable.

4.7. Modeling

The electrochemical potential of the pulp (Eh) is a key factor in the floatability of enargite, as it influences the formation of oxidation products on its surface and, consequently, its interaction with collectors and depressants [39–41,49,73,89,94,104–106]. However, the complexity of mineral systems and the variability of flotation conditions make it difficult to predict electrochemical behavior in industrial environments accurately. Factors such as mineralogical heterogeneity, galvanic interaction with other sulfides, formation of surface species with different degrees of hydrophobicity, and variability in operational conditions significantly influence the flotation response of enargite [35,48,67,68,73,86,89,94,104–106]. Therefore, it is crucial to develop more precise models that simulate the electrochemical response of enargite under different flotation conditions. These models would enable optimization of oxidant and depressant selection and dosage, ensuring more efficient control of the separation process. Additionally, simulating the electrochemical behavior of enargite would facilitate the identification of optimal potential ranges for its selective flotation, minimizing copper losses and reducing the impact of arsenic in concentrates.

4.8. Industrial-Scale Applicability and Challenges

Although laboratory-scale studies have provided valuable insights into the surface chemistry and selective flotation of enargite [3,9,103,105], direct industrial applications remain scarce. The complexity of plant-scale operations, including heterogeneous feed mineralogy, variable pulp chemistry, and operational constraints, poses significant challenges for translating laboratory findings into consistent industrial performance. In particular, maintaining the precise Eh–pH conditions, reagent regimes, and hydrodynamic environments required for selective enargite depression is considerably more difficult in large-scale circuits. Addressing these challenges enables the practical implementation of selective flotation strategies in industrial concentrators, and we identify this gap as a priority research opportunity in the revised outlook section.

Author Contributions: L.G. conceptualized the study, finalized the manuscript; A.R.-M. conceptualized the study, finalized the manuscript; J.H.S. conceptualized the study, finalized the manuscript; R.Y. conceptualized the study, finalized the manuscript; P.M.-V. Developed and analyzed, edited the manuscript. All authors have read and agreed to the published version of the manuscript.

Funding: Water Research Centre for Agriculture and Mining (CRHIAM) projects ANID/FONDAP/15130015 and ANID/FONDAP/1523A0001. Jorge Saavedra thanks project ANID/FONDECYT/11171092.

Data Availability Statement: The original contributions presented in the study are included in the article; further inquiries can be directed to the corresponding author.

Acknowledgments: The authors acknowledge the financial support of the Water Research Centre for Agriculture and Mining (CRHIAM) projects ANID/FONDAP/15130015 and ANID/FONDAP/1523A0001. Jorge Saavedra thanks project ANID/FONDECYT/11171092.

Conflicts of Interest: The authors state that they have no known competing financial interests or personal relationships that could have influenced this paper.

References

1. Long, G.; Peng, Y.; Bradshaw, D. Flotation separation of copper sulphides from arsenic minerals at Rosebery copper concentrator. *Miner. Eng.* **2014**, *66–68*, 207–214. [CrossRef]
2. Plackowski, C.; Nguyen, A.V.; Bruckard, W.J. A critical review of surface properties and selective flotation of enargite in sulphide systems. *Miner. Eng.* **2012**, *30*, 1–11. [CrossRef]
3. Tayebi-Khorami, M.; Manlapig, E.; Forbes, E. Relating the mineralogical characteristics of Tampakan ore to enargite separation. *Minerals* **2017**, *7*, 77. [CrossRef]
4. Biswas, A.K.; Davenport, W.G. *Extractive Metallurgy of Copper*; Pergamon: Oxford, UK, 1994; p. 500.
5. Córdova, R.; Gómez, H.; Real, S.G.; Schrebler, R.; Vilche, J.R. Characterization of natural enargite/aqueous solution systems by electrochemical techniques. *J. Electrochem. Soc.* **1997**, *144*, 2628–2636. [CrossRef]
6. Pineda, D.; Plackowski, C.; Nguyen, A.V. Surface properties of enargite in MAA depressant solutions. *Miner. Eng.* **2015**, *71*, 180–187. [CrossRef]
7. Fornasiero, D.; Fullston, D.; Li, C.; Ralston, J. Separation of enargite and tennantite from non-arsenic copper sulfide minerals by selective oxidation or dissolution. *Int. J. Miner. Process.* **2001**, *61*, 109–119. [CrossRef]
8. Guo, H.; Yen, W.-T. Selective flotation of enargite from chalcopyrite by electrochemical control. *Miner. Eng.* **2005**, *18*, 605–612. [CrossRef]
9. Tayebi-Khorami, M.; Manlapig, E.; Forbes, E.; Bradshaw, D.; Edraki, M. Selective flotation of enargite from copper sulphides in Tampakan deposit. *Miner. Eng.* **2017**, *112*, 1–10. [CrossRef]
10. Yepsen, R.; Gutierrez, L. Effect of Eh and pH on the flotation of enargite using seawater. *Miner. Eng.* **2020**, *159*, 106612. [CrossRef]
11. Henao, J.; de Delgado, G.D.; Delgado, J.; Castrillo, F.; Odreman, O. Single-crystal structure refinement of enargite [Cu_3AsS_4]. *Mater. Res. Bull.* **1994**, *29*, 1121–1127. [CrossRef]
12. Vaughan, D.; Becker, U.; Wright, K. Sulphide mineral surfaces: Theory and experiment. *Int. J. Miner. Process.* **1997**, *51*, 1–14. [CrossRef]
13. Rosso, K.M.; Vaughan, D.J. Sulfide mineral surfaces. *Rev. Miner. Geochem.* **2006**, *61*, 505–556. [CrossRef]
14. Rosso, K.M.; Vaughan, D.J. Reactivity of sulfide mineral surfaces. *Rev. Miner. Geochem.* **2006**, *61*, 557–607. [CrossRef]
15. Rossi, A.; Atzei, D.; Da Pelo, S.; Frau, F.; Lattanzi, P.; England, K.E.R.; Vaughan, D.J. Quantitative X-ray photoelectron spectroscopy study of enargite (Cu_3AsS_4) surface. *Surf. Interface Anal.* **2001**, *31*, 465–470. [CrossRef]
16. Moulder, J.F.; Stickle, W.F.; Sobol, P.E.; Bomben, K.D. *Handbook of X-Ray Photoelectron Spectroscopy*; PHI Division, Perkin Elmer Corporation: Springfield, IL, USA, 1992.
17. Stec, W.J.; Morgan, W.E.; Albridge, R.G.; Van Wazer, J.R. Measured binding energy shifts of the "3p" and "3d" electrons in arsenic compounds. *Inorg. Chem.* **1972**, *11*, 219–225. [CrossRef]
18. Velásquez, P.; Leinen, D.; Pascual, J.; Ramos-Barrado, J.; Cordova, R.; Gómez, H.; Schrebler, R. SEM, EDX and EIS study of an electrochemically modified electrode surface of natural enargite (Cu_3AsS_4). *J. Electroanal. Chem.* **2000**, *494*, 87–95. [CrossRef]
19. Velásquez, P.; Ramos-Barrado, J.R.; Cordova, R.; Leinen, D. XPS analysis of an electrochemically modified electrode surface of natural enargite. *Surf. Interface Anal.* **2000**, *30*, 149–153. [CrossRef]
20. Pratt, A. Photoelectron core levels for enargite, Cu_3AsS_4. *Surf. Interface Anal.* **2004**, *36*, 654–657. [CrossRef]
21. Castillo, I.; Gutierrez, L.; Hernandez, V.; Diaz, E.; Ramirez, A. Hemicelluloses monosaccharides and their effect on molybdenite flotation. *Powder Technol.* **2020**, *373*, 758–764. [CrossRef]
22. Paredes, A.; Acuña, S.M.; Gutiérrez, L.; Toledo, P.G. Zeta Potential of Pyrite Particles in Concentrated Solutions of Monovalent Seawater Electrolytes and Amyl Xanthate. *Minerals* **2019**, *9*, 584. [CrossRef]
23. Fullston, D.; Fornasiero, D.; Ralston, J. Oxidation of synthetic and natural samples of enargite and tennantite: 1. Dissolution and zeta potential study. *Langmuir* **1999**, *15*, 4524–4529. [CrossRef]
24. Buckley, A.; Woods, R. An X-ray photoelectron spectroscopic study of the oxidation of chalcopyrite. *Aust. J. Chem.* **1984**, *37*, 2403–2413. [CrossRef]
25. Chander, S. Electrochemistry of sulfide flotation: Growth characteristics of surface coatings and their properties, with special reference to chalcopyrite and pyrite. *Int. J. Miner. Process.* **1991**, *33*, 121–134. [CrossRef]
26. Fairthorne, G.; Fornasiero, D.; Ralston, J. Effect of oxidation on the collectorless flotation of chalcopyrite. *Int. J. Miner. Process.* **1997**, *49*, 31–48. [CrossRef]

27. Fornasiero, D.; Li, F.; Ralston, J. Oxidation of galena. II. Electrokinetic study. *J. Colloid Interface Sci.* **1994**, *164*, 345–354. [CrossRef]
28. Fornasiero, D.; Li, F.; Ralston, J.; Smart, R.S. Oxidation of galena surface I: X-ray photoelectron spectroscopy and dissolution kinetics studies. *J. Colloid Interface Sci.* **1994**, *164*, 333–344. [CrossRef]
29. Buckley, A.N.; Riley, K.W. Self-induced floatability of sulphide minerals: Examination of recent evidence for elemental sulphur as the hydrophobic entity. *Surf. Interface Anal.* **1991**, *17*, 655–659. [CrossRef]
30. Fullston, D.; Fornasiero, D.; Ralston, J. Zeta potential study of the oxidation of copper sulfide minerals. *Colloids Surf. A* **1999**, *146*, 113–121. [CrossRef]
31. Healy, T.W.; Moignard, M.S. A review of electrokinetic studies of metal sulfides. In *Flotation—A.M. Gaudin Memorial Volume*; Fuerstenau, M.C., Ed.; American Institute of Mining, Metallurgical, and Petroleum Engineers Inc.: New York, NY, USA, 1976; Volume 1, pp. 275–297.
32. Liu, J.C.; Huang, C.P. Electrokinetic characteristics of some metal sulfide-water interfaces. *Langmuir* **1992**, *8*, 1851–1856. [CrossRef]
33. Fullston, D.; Fornasiero, D.; Ralston, J. Oxidation of synthetic and natural samples of enargite and tennantite: 2. X-ray photoelectron spectroscopic study. *Langmuir* **1999**, *15*, 4530–4536. [CrossRef]
34. Cordova, R.; Gomez, H.; Schrebler, R.; Real, S.G.; Vilche, J.R. An electrochemical study of enargite in aqueous solutions by transient techniques. In *Proceedings—Electrochemical Society: 96–6 (Electrochemistry in Mineral and Metal Processing)*; The Electrochemical Society: Pennington, NJ, USA, 1996; pp. 356–367.
35. Castro, S.H.; Honores, S. Surface properties and floatability of enargite. In Proceedings of the XXI International Mineral Processing Conference, Rome, Italy, 23–27 July 2000; Massacci, P., Ed.; Elsevier Science B.V.: Rome, Italy, 2000; pp. B8b-47–B8b-53.
36. Schwedt, G.; Rieckhoff, M. Separation of thio- and oxothioarsenates by capillary zone electrophoresis and ion chromatography. *J. Chromatogr. A* **1996**, *736*, 341–350. [CrossRef]
37. Plackowski, C.; Hampton, M.A.; Bruckard, W.J.; Nguyen, A.V. An XPS investigation of surface species formed by electrochemically induced surface oxidation of enargite in the oxidative potential range. *Miner. Eng.* **2014**, *55*, 60–74. [CrossRef]
38. Castro, S.; Baltierra, L. Study of the surface properties of enargite as a function of pH. *Int. J. Miner. Process.* **2005**, *77*, 104–115. [CrossRef]
39. Plackowski, C.; Bruckard, W.J.; Nguyen, A.V. Surface characterisation, collector adsorption and flotation response of enargite in a redox potential controlled environment. *Miner. Eng.* **2014**, *65*, 61–73. [CrossRef]
40. Pauporté, T.; Schuhmann, D. An electrochemical study of natural enargite under conditions relating to those used in flotation of sulphide minerals. *Colloids Surf. A* **1996**, *111*, 1–19. [CrossRef]
41. Ma, Y.; Yang, Y.; Skinner, W.; Chen, M. Electrochemical and spectroscopic analysis of enargite (Cu_3AsS_4) dissolution mechanism in sulfuric acid solution. *Hydrometallurgy* **2020**, *194*, 105346. [CrossRef]
42. Ásbjörnsson, J.; Kelsall, G.H.; Pattrick, R.A.D.; Vaughan, D.J.; Wincott, P.L.; Hope, G.A. Electrochemical and surface analytical studies of enargite in acid solution. *J. Electrochem. Soc.* **2004**, *151*, E250–E256. [CrossRef]
43. Guo, H.; Yen, W.T. Electrochemical study of synthetic and natural enargites. In Proceedings of the 24th International Mineral Processing Congress, Beijing, China, 24–28 September 2008; Volume 1, pp. 1138–1145.
44. Lattanzi, P.; Da Pelo, S.; Musu, E.; Atzei, D.; Elsener, B.; Fantauzzi, M.; Rossi, A. Enargite oxidation: A review. *Earth-Sci. Rev.* **2008**, *86*, 62–88. [CrossRef]
45. Sasaki, K.; Takatsugi, K.; Ishikura, K.; Hirajima, T. Spectroscopic study on oxidative dissolution of chalcopyrite, enargite and tennantite at different pH values. *Hydrometallurgy* **2010**, *100*, 144–151. [CrossRef]
46. Welham, N. Mechanochemical processing of enargite (Cu_3AsS_4). *Hydrometallurgy* **2001**, *62*, 165–173. [CrossRef]
47. Plackowski, C.; Hampton, M.A.; Nguyen, A.V.; Bruckard, W.J. Fundamental studies of electrochemically controlled surface oxidation and hydrophobicity of natural enargite. *Langmuir* **2013**, *29*, 2371–2386. [CrossRef] [PubMed]
48. García-Garnica, R.; Castillo-Magallanes, N.; Rodríguez, I.; Cruz, R.; Lázaro, I. Electrochemical study of enargite within the mixed potential zone attained with different oxidizing reagents in an alkaline medium. *Electrochim. Acta* **2022**, *425*, 140719. [CrossRef]
49. Gow, R.N.; Young, C.; Huang, H.; Hope, G. Spectroelectrochemistry of enargite III: Alkaline sulfide leaching. *Min. Met. Explor.* **2015**, *32*, 14–21. [CrossRef]
50. Guo, H.; Yen, W.-T. Surface potential and wettability of enargite in potassium amyl xanthate solution. *Miner. Eng.* **2002**, *15*, 405–414. [CrossRef]
51. Guo, B.H.; Yen, W.-T. Electrochemical investigation on wettability of enargite. In Proceedings of the Interactions in Mineral Processing the Fourth UBC-McGill International Symposium on Fundamentals of Mineral Processing as held at the 40th Annual Conference of Metallurgists of CIM(COM 2001), Toronto, ON, Canada, 26–29 August 2001; pp. 325–336.
52. Gan, Y.; Deng, R.; Liu, Q. Flotation separation of covellite and enargite via oxidation treatment. *Minerals* **2022**, *12*, 970. [CrossRef]
53. Chau, T.T.; Bruckard, W.J.; Koh, P.T.L.; Nguyen, A.V. A review of factors that affect contact angle and implications for flotation practice. *Adv. Colloid Interface Sci.* **2009**, *150*, 106–115. [CrossRef]
54. Bhushan, B.; Jung, Y.C.; Koch, K. Micro-, nano- and hierarchical structures for superhydrophobicity, self-cleaning and low adhesion. *Philos. Trans. R. Soc. A* **2009**, *367*, 1631–1672. [CrossRef]

55. Ma, X.; Bruckard, W. Rejection of arsenic minerals in sulfide flotation—A literature review. *Int. J. Miner. Process.* **2009**, *93*, 89–94. [CrossRef]
56. Tajadod, J.; Yen, W.T. Arsenic content reduction in copper concentrates. In Proceedings of the 2nd UBC-McGill Bi-Annual International Symposium on Fundamental Mineral Processing: Processing of Complex Ores, Sudbury, ON, Canada, 17–19 August 1997; pp. 153–164.
57. Nishimura, T.; Itoh, C.T.; Tozawa, K. Stabilities and solubilities of metal arsenites and arsenates in water and effect of sulfate and carbonate ions on their solubilities. In *Arsenic Metallurgy Fundamentals and Application*; Reddy, R.G., Hendrix, J.L., Queneau, P.B., Eds.; TMS: Warrendale, PA, USA, 1988; pp. 77–98.
58. Yen, W.T.; Tajadod, J. Selective flotation of enargite and chalcopyrite. In Proceedings of the XXI International Mineral Processing Conference, Rome, Italy, 23–27 July 2000; Volume B, pp. B8a-49–B8a-55.
59. Castro, S.H.; Baltierra, L.; Muñoz, P. Depression of enargite by magnesium-ammonium mixtures. In Proceedings of the Copper 2003–Cobre 2003, the 5th International Conference, Santiago, Chile, 30 November–3 December 2003; Volume III, pp. 257–269.
60. Dai, Z.; Garritsen, J.; Wells, P.F.; Xu, M. Arsenic rejection in the flotation of Garson Ni–Cu ore. In Proceedings of the Centenary of Flotation Symposium, Brisbane, Australia, 5–9 June 2005; pp. 939–946.
61. Tapley, B.; Yan, D. The selective flotation of arsenopyrite from pyrite. *Miner. Eng.* **2003**, *16*, 1217–1220. [CrossRef]
62. Tajadod, J.; Yen, W.T. A comparison of surface properties and flotation characteristics of enargite and chalcopyrite. In Proceedings of the XX International Mineral Processing Congress, Aachen, Germany, 21–26 September 1997; Volume 3, pp. 409–418.
63. Tajadod, J. A laboratory study of removing arsenic from a synthetic copper concentrate. *Int. J. Eng.* **2000**, *13*, 1–10.
64. Suyantara, G.P.W.; Hirajima, T.; Miki, H.; Sasaki, K.; Kuroiwa, S.; Aoki, Y. Effect of Na_2SO_3 on the floatability of chalcopyrite and enargite. *Miner. Eng.* **2021**, *173*, 107222. [CrossRef]
65. Suyantara, G.P.W.; Hirajima, T.; Miki, H.; Sasaki, K.; Kuroiwa, S.; Aoki, Y. Effect of H_2O_2 and potassium amyl xanthate on separation of enargite and tennantite from chalcopyrite and bornite using flotation. *Miner. Eng.* **2020**, *152*, 106371. [CrossRef]
66. Lin, R.; Liu, Q.; Deng, R. Calcium lignosulfonate as a depressant for enhancing flotation separation of covellite and enargite. *Min. Met. Explor.* **2024**, *41*, 1135–1144. [CrossRef]
67. Hu, Y.H.; Qiu, G.H.; Sun, S.Y.; Wang, D.Z. Recent development in researches of electrochemistry of sulfide flotation at Central South University of Technology. *Trans. Met. Soc. China* **2000**, *10*, 1–7.
68. Kantar, C. Solution and flotation chemistry of enargite. *Colloids Surf. A* **2002**, *210*, 23–31. [CrossRef]
69. Luttrell, G.H.; Yoon, R.-H. The collectorless flotation of chalcopyrite ores using sodium sulfide. *Int. J. Miner. Process.* **1984**, *13*, 271–283. [CrossRef]
70. Pang, J.; Chander, S. Oxidation and wetting behavior of chalcopyrite in the absence and presence of xanthates. *Min. Met. Explor.* **1990**, *7*, 149–155. [CrossRef]
71. Qin, W.Q.; Qiu, G.Z.; Xu, J. Electrodeposition of dixanthogen on surface of pyrrhotite electrode. *Trans. Met. Soc. China* **2000**, *10*, 61–63.
72. Rao, S.R.; Finch, J.A. Galvanic interactions studies on sulfide minerals. *Can. Met. Q.* **1988**, *27*, 253–259. [CrossRef]
73. Trahar, W.; Senior, G.; Shannon, L. Interactions between sulfide minerals—The collectorless flotation of pyrite. *Int. J. Miner. Process.* **1994**, *40*, 287–321. [CrossRef]
74. Guo, H.; Yen, W.T. Electrochemical floatability of enargite and effects of depressants. In Proceedings of the XXIII International Mineral Processing Conference, Istanbul, Turkey, 3–8 September 2006; pp. 504–509.
75. Senior, G.; Guy, P.; Bruckard, W. The selective flotation of enargite from other copper minerals—A single mineral study in relation to beneficiation of the Tampakan deposit in the Philippines. *Int. J. Miner. Process.* **2006**, *81*, 15–26. [CrossRef]
76. Bruckard, W.; Kyriakidis, I.; Woodcock, J. The flotation of metallic arsenic as a function of pH and pulp potential—A single mineral study. *Int. J. Miner. Process.* **2007**, *84*, 25–32. [CrossRef]
77. Bruckard, W.; Davey, K.; Jorgensen, F.; Wright, S.; Brew, D.; Haque, N.; Vance, E. Development and evaluation of an early removal process for the beneficiation of arsenic-bearing copper ores. *Miner. Eng.* **2010**, *23*, 1167–1173. [CrossRef]
78. Smith, L.K.; Heyes, G.W. The effect of water quality on the collectorless flotation of chalcopyrite and bornite. In Proceedings of the 3rd International Congress on Water Management in the Mining Industry, Santiago, Chile, 6–8 June 2012.
79. Smith, L.; Bruckard, W. The separation of arsenic from copper in a Northparkes copper–gold ore using controlled-potential flotation. *Int. J. Miner. Process.* **2007**, *84*, 15–24. [CrossRef]
80. Kappes, R.; Gathje, J. The metallurgical development of an enargite-bearing deposit. In Proceedings of the XXV International Mineral Processing Congress (IMPC), Brisbane, QLD, Australia, 6–10 September 2010.
81. Runge, K. Laboratory flotation testing—An essential tool for ore characterisation. In *Flotation Plant Optimisation: A Metallurgical Guide to Identifying and Solving Problems in Flotation Plants*; Greet, C.J., Ed.; Australasian Institute of Mining and Metallurgy: Carlton, VIC, Australia, 2010.
82. Tayebi-Khorami, M.; Manlapig, E.; Forbes, E.; Edraki, M.; Bradshaw, D. Effect of surface oxidation on the flotation response of enargite in a complex ore system. *Miner. Eng.* **2018**, *119*, 149–155. [CrossRef]

83. Azizi, A.; Shafaei, S.Z.; Noaparast, M.; Karamoozian, M.; Ibric, S. Galvanic interaction between chalcopyrite and pyrite with low alloy and high carbon chromium steel ball. *J. Chem.* **2013**, 817218. [CrossRef]
84. Ekmekçi, Z.; Demirel, H. Effects of galvanic interaction on collectorless flotation behaviour of chalcopyrite and pyrite. *Int. J. Miner. Process.* **1997**, *52*, 31–48. [CrossRef]
85. Huang, G.; Grano, S. Galvanic interaction of grinding media with pyrite and its effect on flotation. *Miner. Eng.* **2005**, *18*, 1152–1163. [CrossRef]
86. Martin, C.; Rao, S.; Finch, J.; Leroux, M. Complex sulphide ore processing with pyrite flotation by nitrogen. *Int. J. Miner. Process.* **1989**, *26*, 95–110. [CrossRef]
87. Peng, Y.; Grano, S.; Fornasiero, D.; Ralston, J. Control of grinding conditions in the flotation of chalcopyrite and its separation from pyrite. *Int. J. Miner. Process.* **2003**, *69*, 87–100. [CrossRef]
88. Rabieh, A.; Albijanic, B.; Eksteen, J. A review of the effects of grinding media and chemical conditions on the flotation of pyrite in refractory gold operations. *Miner. Eng.* **2016**, *94*, 21–28. [CrossRef]
89. Bradshaw, D.; Buswell, A.; Harris, P.; Ekmekci, Z. Interactive effects of the type of milling media and copper sulphate addition on the flotation performance of sulphide minerals from Merensky ore Part I: Pulp chemistry. *Int. J. Miner. Process.* **2006**, *78*, 153–163. [CrossRef]
90. Jacques, S.; Greet, C.; Bastin, D. Oxidative weathering of a copper sulphide ore and its influence on pulp chemistry and flotation. *Miner. Eng.* **2016**, *99*, 52–59. [CrossRef]
91. Chen, X.; Peng, Y.; Bradshaw, D. The separation of chalcopyrite and chalcocite from pyrite in cleaner flotation after regrinding. *Miner. Eng.* **2014**, *58*, 64–72. [CrossRef]
92. Cheng, X.; Iwasaki, I. Pulp potential and its implications to sulphide flotation. *Miner. Process. Extr. Met. Rev.* **1992**, *11*, 187–210. [CrossRef]
93. Hu, Y.; Sun, W.; Wang, D. *Electrochemistry of Flotation of Sulphide Minerals*; Springer: Berlin/Heidelberg, Germany, 2009.
94. Rao, S.R.; Labonte, G.; Finch, I.A. Electrochemistry in the plant. In *Innovations in Flotation Technology*; Marvos, P., Matis, K.A., Eds.; Kluwer Academic: Dordrecht, The Netherlands, 1992.
95. Grano, S.; Lauder, D.; Johnson, N.; Ralston, J. An investigation of galena recovery problems in the Hilton concentrator of Mount Isa Mines Limited, Australia. *Miner. Eng.* **1997**, *10*, 1139–1163. [CrossRef]
96. Greet, C.J. The significance of grinding environment on the flotation of UG2 ores. *J. S. Afr. Inst. Min. Metall.* **2009**, *109*, 37–42.
97. Peng, Y.; Grano, S.; Fornasiero, D.; Ralston, J. Control of grinding conditions in the flotation of galena and its separation from pyrite. *Int. J. Miner. Process.* **2003**, *70*, 67–82. [CrossRef]
98. Rumball, J.; Richmond, G. Measurement of oxidation in a base metal flotation circuit by selective leaching with EDTA. *Int. J. Miner. Process.* **1996**, *48*, 1–20. [CrossRef]
99. Senior, G.; Trahar, W. The influence of metal hydroxides and collector on the flotation of chalcopyrite. *Int. J. Miner. Process.* **1991**, *33*, 321–341. [CrossRef]
100. Smart, R. Surface layers in base metal sulphide flotation. *Miner. Eng.* **1991**, *4*, 891–909. [CrossRef]
101. Huch, R.O.; Cyprus Mineral Company. Method for Achieving Enhanced Copper-Containing Mineral Concentrate Grade by Oxidation and Flotation. US Patent 5,295,585, 22 March 1994.
102. Marasinghe, B.; Koleini, S.M. Separation of arsenic from mining and metallurgical wastes. In Proceedings of the Australasian Institute of Mining and Metallurgy Student Conference, Brisbane, QLD, Australia, 28–29 April 1994; pp. 93–98.
103. Li, T.; Zhang, Y.; Zhang, B.; Jiao, F.; Qin, W. Flotation separation of enargite from complex copper concentrates by selective surface oxidation. *Physicochem. Probl. Miner. Process.* **2019**, *55*, 852–864. [CrossRef]
104. Petrus, H.T.; Hirajima, T.; Sasaki, K.; Okamoto, H. Effects of sodium thiosulphate on chalcopyrite and tennantite: An insight for alternative separation technique. *Int. J. Miner. Process.* **2012**, *102–103*, 116–123. [CrossRef]
105. Suyantara, G.P.W.; Miki, H.; Hirajima, T.; Sasaki, K.; Ochi, D.; Aoki, Y. Selective flotation of copper concentrates containing arsenic minerals using potassium amyl xanthate and oxidation treatment. *Mater. Trans.* **2024**, *65*, 27–36. [CrossRef]
106. Suyantara, G.P.W.; Berdakh, D.; Miki, H.; Hirajima, T.; Sasaki, K.; Ochi, D.; Aoki, Y. Effect of hydrogen peroxide on selective flotation of chalcocite and enargite. *Int. J. Min. Sci. Technol.* **2023**, *33*, 703–716. [CrossRef]
107. Castro, S.; Laskowski, J.S. Froth flotation in saline water. *KONA Powder Part. J.* **2011**, *29*, 4–15. [CrossRef]
108. Castro, S.; Uribe, L.; Laskowski, J.S. Depression of inherently hydrophobic minerals by hydrolysable metal cations: Molybdenite depression in seawater. In Proceedings of the 27th International Mineral Processing Congress (IMPC), Santiago, Chile, 20–24 October 2014; pp. 207–217.
109. Rebolledo, E.; Laskowski, J.S.; Gutierrez, L.; Castro, S. Use of dispersants in flotation of molybdenite in seawater. *Miner. Eng.* **2017**, *100*, 71–74. [CrossRef]
110. Yepsen, R.; Gutierrez, L.; Laskowski, J. Flotation behavior of enargite in the process of flotation using seawater. *Miner. Eng.* **2019**, *142*, 105897. [CrossRef]

111. Raposo, J.C.; Zuloaga, O.; Olazabal, M.A.; Madariaga, J.M. Study of the precipitation equilibria of arsenate anion with calcium and magnesium in sodium perchlorate at 25 °C. *Appl. Geochem.* **2004**, *19*, 855–862. [CrossRef]
112. Li, C.; Somasundaran, P. Reversal of bubble charge in multivalent inorganic salt solutions—Effect of magnesium. *J. Colloid Interface Sci.* **1991**, *146*, 215–218. [CrossRef]
113. Dávila-Pulido, G.; Uribe-Salas, A.; Álvarez-Silva, M.; López-Saucedo, F. The role of calcium in xanthate adsorption onto sphalerite. *Miner. Eng.* **2015**, *71*, 113–119. [CrossRef]
114. Sigauke, T.; Johnson, O.T.; Ndeshimona, V.L.; Mashingaidze, M.M. Advancements in nanotechnology for the enhanced flotation of fine mineral particles: A review. *Discov. Appl. Sci.* **2025**, *7*, 317. [CrossRef]
115. Wang, D.; Liu, Q. Hydrodynamics of froth flotation and its effects on fine and ultrafine mineral particle flotation: A literature review. *Miner. Eng.* **2021**, *173*, 107220. [CrossRef]